VIRAL IMMUNOLOGY
Volume 22, Number 6, 2009

Pp. 353–369
DOI: 10.1089/vim.2009.0057

IFN-β-Induced Alteration of VSV Protein Phosphorylation in Neuronal Cells

Paul M. D'agostino,[1] Jessica J. Amenta,[1] and Carol Shoshkes Reiss[1–5]

Abstract

Vesicular stomatitis virus (VSV) replication is highly sensitive to interferon (IFN)-induced antiviral responses. VSV infection of well-known cell lines pretreated with IFN-β results in a 10^4-fold reduction in the release of infectious particles, with a concomitant abrogation in viral transcript and/or protein levels. However, in cell lines of neuronal lineage only a threefold reduction in viral transcript and protein levels was observed, despite the same 10^4-fold reduction in released infectious virions, suggesting an assembly defect. Examination of VSV matrix (M) protein ubiquitination yielded no differences between mock- and IFN-β-treated neuronal cells. Further analysis of potential post-translational modification events, by scintillation and two-dimensional electrophoretic methods, revealed IFN-β-induced alterations in M protein and phosphoprotein (P) phosphorylation. Hypophosphorylated P protein was demonstrated by reduced ^{32}P counts, normalized by ^{35}S-cysteine/methionine incorporation, and by a shift in isoelectric focusing. Hypophosphorylation of VSV P protein was found to occur in neuronal cell lysates, but not within budded virions from the same IFN-β-treated cells. In contrast, hyperphosphorylation of VSV M protein was observed in both cell lysates and viral particles from IFN-β-treated neuronal cells. Hyperphosphorylated M protein was demonstrated by increased ^{32}P counts relative to ^{35}S-cysteine/methionine normalization, and by altered isoelectric focusing in protein populations from cell and viral lysates. Hyperphosphorylated VSV M protein was found to inhibit its association with VSV nucleocapsid, suggesting a possible mechanism for type I IFN-mediated misassembly through disruption of the interactions between ribonucleoprotein cores, and hyperphosphorylated M protein bound to the plasma membrane inner leaflet.

Introduction

Given the immunological privilege associated with the central nervous system (CNS), neurons must rely heavily on innate immunity when dealing with viral pathogens. Among the known cell autonomous innate immune responses, the interferon (IFN) pathway is considered to be crucial to fighting viral infections (15,23,36). The use of vesicular stomatitis virus (VSV) as a model pathogen, due to its high sensitivity to IFN-elicited responses, has been well documented both *in vitro* and in mice (37,55).

VSV is a member of the Rhabdoviridae family, and is a bullet-shaped, enveloped, negative sense, single-stranded RNA virus. Within the VSV genome there are five annotated viral gene products: nucleocapsid (N), matrix (M), glycoprotein (G), phosphoprotein (P), and the large subunit (L). The VSV P and L proteins together form a functional RNA-dependent RNA polymerase (RDRP) (10,11,15,31,46). This RDRP alternatively synthesizes viral mRNA transcripts and replicates the VSV genome through variably phosphorylated serines and threonines located in both the amino- and carboxy-terminal domains of VSV P (1,2,8,9,31).

Type I IFNs (e.g., IFN-α and IFN-β) are induced in mice infected intravenously, intraperitoneally, or intranasally with VSV, leading to effective clearance of the pathogen (30,43,51,54). Disruption of the type I IFN pathway results in severe host compromise and rapid death from VSV infection (13,14,30,43). Intranasal VSV infection leads to encephalitis without type I IFN production within the CNS, even though it is readily observed in peripheral lymphoid tissues at 24 h post-infection (32,51). Type I IFN present in the periphery is unable to cross the blood–brain barrier and inhibit VSV replication in the CNS (7). No induction of IFN expression was found in studies of VSV-infected primary neurons *ex vivo* or neuroblastoma cell lines *in vitro* (52). However, when these cells are pretreated with IFN-β prior to VSV infection, a

[1]Biology Department, [2]Center for Neural Science, [3]Microbiology Department, and [4]NYU Cancer Center, New York University, New York, New York.
[5]Microbiology Department, Mount Sinai School of Medicine, New York, New York.

profound attenuation in the release of infectious particles is observed; an abrogation largely independent of any inhibition to viral translation, transcription, and viral genomic replication (52). Furthermore, VSV infection in the presence of IFN-β and specific inhibitors of well characterized IFN-dependent antiviral effector pathways (e.g., protein kinase R or nitric oxide synthase-1) has no effect on the efficacy of IFN treatment, indicating suppression of viral replication by other pathways (52).

Non-traditional actions associated with an IFN antiviral response have been reported for RNA tumor viruses and Ebola virus (45,57), as well as for vesicular stomatitis virus (41). In each case, the general phenomenon observed pertained to a drop in production of infectious virions (in some cases without a significant drop in total viral particles) without inhibition at the viral transcript or viral protein level. Although these observations were not made in neurons, they did imply an ability of IFN to inhibit a late stage of the viral infectious cycle.

The endosomal sorting complex for transport (ESCRT) pathway is most known for its ability to sort mono-ubiquitinated proteins for lysosomal degradation (48). ESCRT pathway components have also been implicated in membrane abscission events that are topologically inverted from those used for endocytic vesicle formation (e.g., cytokinesis and viral budding) (18,48). Current evidence for enveloped viruses that bud from the plasma membrane (such as retroviruses, filoviruses, and rhabdoviruses) shows their ability to utilize interactions between "late" domain motifs found within viral structural proteins, and WW-domain containing E3 ubiquitin ligases, as well as ESCRT I and III complex subunits (TSG101 and VPS4), to facilitate the budding of viral progeny (18,50).

For VSV, it is the M protein that plays a pivotal role in viral assembly though interactions between its "late" domains (PPXY, PT/SAP, and YXXL), and ESCRT pathway components (27). Nedd4, a membrane-bound WW domain containing E3 ubiquitin ligase, has been shown to both interact with and ubiquitinate M in a PPXY-dependent manner (33). Furthermore, mutations in the PPXY domain lead to inhibition in budding activities with M protein transfected alone in cells (28), and when expressed in infectious particles (34). Therefore if a type I IFN response in neurons leads to misassembled virions, assessing any changes in M protein ubiquitination would be logical.

Given our previous observations made in neuronal cells, as well as published findings in other cell types, we sought to answer the following questions: (1) are there differences between a neuronal- and non-neuronal-derived IFN response, as it pertains to the VSV infection cycle?; and, (2) do such alterations effect VSV assembly? Our experiments have been designed to examine any differences in VSV protein post-translational modification, due to an IFN-elicited response, that may contribute directly or indirectly to impaired virion assembly. To that end, we have focused our efforts on post-translational modifications previously shown to be essential during the VSV infectious cycle, namely ubiquitination and phosphorylation.

Materials and Methods

Cell lines, virus, and general reagents

NB41A3 neuroblastoma cells (ATCC CCL-147; Manassas, VA), NIH/3T3 (ATCC CRL-1658), and L929 (ATCC CCL-1) were cultured as previously described (52). VSV Indiana strain, San Juan serotype, was originally obtained from Alice S. Huang (then at The Children's Hospital, Boston, MA). Murine IFN-β (R&D Systems, Minneapolis, MN), ^{32}P-orthophosphate (Perkin Elmer, Waltham, MA), ^{35}S-cysteine/methionine (Perkin Elmer), and 2,5-diphenyloxazole (PPO; Sigma-Aldrich, St. Louis, MO) were used.

Cells and viral particles were lysed with radio-immunoprecipitation (RIP) buffer, defined as follows: 20 mM Tris (pH 7.4), 0.5 M NaCl, 200 mM NaF, 30 mM NaH_2PO_4, 5 mM EDTA, 0.5% NP-40, 0.02% NaN_3, 2 mM Na_3VO_4, 2 mM PMSF, 1 μg/mL pepstatin, 0.5 μg/mL leupeptin, and 2 μg/mL aprotinin. The RIP wash buffer used during immunoprecipitations consisted of PBS + 0.5% NP-40. Gel electrophoresis used acrylamide solutions (Bio-Rad, Hercules, CA) with either a 37.5:1 or a 19:1 acrylamide:bisacrylamide ratio; a pH 3–10 ampholyte solution (Bio-Rad) was used for two-dimensional gels via the Mini-Protean 2-D Tube Gel Kit (Bio-Rad).

Tissue culture was done using complete medium of either F12K (Mediatech, Herndon, VA) or DMEM (Mediatech) supplemented with donor horse serum (Mediatech) and/or fetal bovine serum (Atlanta Biologicals, Lawerenceville, GA), in addition to other cell-line-specific supplements cited by ATCC. Lastly, viral plaque assays and Western blots were performed as previously described (52).

Infections and radiolabeling for harvesting cell and viral lysates from neuronal and non-neuronal cells

VSV infections were carried out in NB41A3, L929, and NIH3T3 cells either treated with 400 U/mL IFN-β or medium alone for 18–24 h prior to infection. VSV was always added to cells in serum-free media, at a multiplicity of infection (MOI) equal to 3 (MOI = 3), and allowed to incubate for 30 min at 37°C in 5% CO_2. Subsequently unbound virus was removed by washing the monolayer several times with sterile HBSS (Mediatech), and it was re-fed with complete media for the duration of the infection.

Several radiolabeling techniques were employed in this article. For experiments using a single label (either 50 μCi/mL ^{32}P-orthophosphate or 125 μCi/mL ^{35}S-cysteine/methionine), a growth medium was used throughout the infection that was deficient in non-radiological sources of that isotope (i.e., phosphate-free DMEM [MP Biomedicals, Solon, OH], or DMEM without L-cysteine, L-methionine, and L-glutamine [Mediatech]). When fully supplemented medium was called for to propagate viral infections, the chosen medium was supplemented with an HBSS-dialyzed (molecular weight cut-off 12–14 kDa) preparation of 15% donor horse serum and 2.5% fetal bovine serum, in addition to other cell-line-specific supplements cited by ATCC. For experiments using dual-labeling (50 μCi/mL ^{32}P-orthophosphate and 125 μCi/mL ^{35}S-cysteine/methionine), phosphate-free DMEM was always used as the base medium.

To generate cell lysates, at 6 h post-infection (hpi) supernatants were harvested for plaque assay, centrifuged at 1700 relative centrifugal force (RCF) for 10 min to remove cellular debris, and stored at −80°C. The remaining cells were then washed once with excess HBSS and lysed in 500 μL of RIP buffer (containing protease and phosphatase inhibitors) for 10–15 min, centrifuged at 14,000 RCF for 10 min to remove insoluble debris, and stored at −80°C.

To generate viral lysates, viral supernatants were harvested at 10 hpi to collect released virions, followed by an initial centrifugation at 1700 RCF for 10 min to remove cell debris. Afterwards, the clarified supernatants were transferred to ultracentrifuge tubes and VSV virions were pelleted at 300,000 RCF for 15 min. Viral pellets were then washed once in excess HBSS, repelleted, and lysed in 100 μL of RIP buffer supplemented with protease and phosphatase inhibitors.

Standard immunoprecipitations followed by scintillation analysis

VSV-infected single or dual metabolically-labeled cell lysates, derived from both control and IFN-β-treated cells, were mixed with either 1:100 rabbit anti-VSV P antiserum (a gift from Gail Wertz [25]), 20 μg/mL mouse anti-VSV M 23H12 monoclonal antibody (a gift from Doug Lyles [38]), or 1:100 sheep anti-VSV antiserum (a gift from Alice S. Huang [40]). Antigen-antibody complexes were precipitated with either 1:10 Pansorbin® A Cells (Calbiochem, San Diego, CA), or 25 μL packed Protein A/G agarose beads (Pierce division of Thermo Scientific, Rockford, IL), depending on the species of the primary antibody. The pellets were washed twice with RIP lysis buffer and once with an RIP wash buffer. The washed pellets were resuspended in sample buffer (0.05% bromophenol blue, 62.5 mM Tris [pH 6.8], 1% SDS, 10% glycerol, and 100 mM dithiothreitol) and denatured at 100°C for 5 min. Dissociated protein samples were then resolved via 12% (16-cm gel) SDS-PAGE, and stained with Coomassie Brilliant Blue R250 (Sigma-Aldrich).

For scintillation analysis of dual-labeled samples, the gels were then wrapped in plastic wrap and exposed to film overnight at 25°C. The developed film, along with Coomassie-stained bands, were used to excise bands corresponding to VSV P or M proteins; these bands were then dissolved (24). Briefly, excised bands were placed in a 1-mL solution of 30% H_2O_2 (Fisher, Waltham, MA) and concentrated NH_4Cl (Sigma-Aldrich), and incubated at 60°C for 24–48 h. Entire volumes of dissolved bands were then mixed separately 1:5 with Ready Protein$^+$ scintillation fluid (Beckman Coulter, Fullerton, CA), and $^{35}S/^{32}P$ counts detected with a Beckman LS6000LL scintillation counter. Viral lysates were not immunoprecipitated, but were denatured at 100°C for 5 min in sample buffer, loaded at fixed volumes (50 μL) per well, resolved via 12% (16-cm gel) SDS-PAGE, and treated as described above.

Detecting ubiquitinated VSV M protein by "double" immunoprecipitations of NB41A3 cell lysates

VSV-infected ^{35}S-cysteine/methionine-labeled cell lysates, derived from both control and IFN-β-treated cells, were first treated with a 1:100 dilution of both sheep polyclonal anti-VSV anti-serum and rabbit polyclonal anti-GAPDH antibody (Abcam, Cambridge, MA). Using the standard immunoprecipitation protocol detailed above, antigen-antibody complexes were precipitated with Pansorbin A cells (Fisher), the only difference being that washed pellets were denatured at 100°C for 5 min in 1% SDS + PBS. The resulting VSV/GAPDH-enriched protein solutions were diluted in 300 μL RIP buffer (to nullify the effects of the SDS), and were again immunoprecipitated, this time with a 1:100 dilution of rabbit polyclonal anti-ubiquitin (Abcam) and polyclonal anti-GAPDH antibodies. Experimental samples were then denatured at 100°C for 5 min in sample buffer, and resolved via 14% (8-cm gel) SDS-PAGE.

In preparation for autoradiography, the gels were washed two times with excess DMSO for 30 min, followed by treatment with 22% PPO_{DMSO} overnight. The gels were subsequently rehydrated for 30 min, and dried for 2 h at 80°C using a Savant Speed Gel SG210D. The dried gels were then exposed to film for varying times at −80°C to ensure that the autoradiographs contained bands within a linear range for densitometry analysis using UN-SCAN-IT^{TM} Gel software version 5.1.

Sequential immunoprecipitations, autoradiography, and densitometry of NB41A3 cell lysates

VSV-infected ^{35}S-cysteine/methionine-labeled cell lysates, derived from both control and IFN-β-treated cells, were first treated (100 μL) with either rabbit anti-P antiserum (1:100), rabbit anti-N antiserum (1:100) (25), or mouse anti-M monoclonal 23H12 antibody (20 μg/mL) and incubated for 24 h at 4°C. Using the standard immunoprecipitation protocol detailed above, antigen-antibody complexes were precipitated with Pansorbin A cells. The supernatants were carefully transferred to a new tube for subsequent rounds of immunoprecipitations. The same protocol was carried out three more times on the cell lysate samples saved from the first precipitation, taking into account changes in volume due to antibody and Pansorbin additions.

After the fourth precipitation any unbound viral proteins were treated with sheep anti-VSV antiserum (1:100) for 24 h at 4°C, followed by precipitation with 25 μL of packed Protein A/G agarose beads (Pierce), and rotated at room temperature for 1 h. All precipitated pellets were treated as described above in the standard immunoprecipitation protocol. Denatured protein samples were then resolved via 14% (8-cm gel) SDS-PAGE and processed for autoradiography as described above.

Autoradiography and densitometry on viral proteins incorporated into virions

^{35}S-cysteine/methionine-labeled viral lysates, derived from both control and IFN-β-treated cells, were analyzed by scintillation counter, normalized to 20,000 CPM, and denatured at 100°C for 5 min in sample buffer. Denatured protein samples were then resolved via 12% (16-cm gel) SDS-PAGE, and processed for autoradiography as described above. Densitometry values were subsequently analyzed by taking all possible ratio permutations for virion-associated proteins and comparing them between each treatment group.

Two-dimensional electrophoresis of VSV proteins in cell lysates and from viral particle budded from NB41A3 cells

VSV-infected, ^{35}S-cysteine/methionine-labeled cell lysates, derived from both control and IFN-β-treated cells, were immunoprecipitated with sheep anti-VSV antiserum as described above. Denaturation was carried out at room temperature using a milder solution (4 M urea, 1% Triton X-100, 2.5% β-mercaptoethanol, 0.01% bromophenol blue, and

0.01% methylene red) supplemented with ampholytes. Denatured samples were then subjected to capillary gel isoelectric focusing across a pH 3–10 ampholyte gradient (Bio-Rad) composed of 5% polyacrylamide. Following isoelectric focusing, capillary gels were extruded, further resolved via 14% (8-cm gel) SDS-PAGE, and processed for autoradiography as described above. Samples representing VSV-infected, ^{35}S-cysteine/methionine-labeled viral lysates, derived from both control and IFN-β-treated cells, were normalized to 25,000 CPM, denatured, and processed similarly to the cell lysates.

Statistical analyses

All experimental samples were prepared in triplicate, in at least three separate experiments. Data points representing more than two standard deviations from the mean, or within two standard deviations of background, were culled from data sets. Sample *t*-values were calculated using Satterthwaite's method for independent samples of unequal variances, and hypothesis testing was employed to determine whether or not quantities (e.g., ^{35}S:^{32}P ratios) were equal, yielding *p*-values indicative of these tests. All error bars represent 95% confidence intervals of a particular data set unless otherwise stated.

Results

IFN responses to VSV infections in NB41A3 neuroblastomas differ from those in NIH/3T3 or L929 fibroblast-derived cell lines

NIH/3T3 and L929 are two mouse fibroblast-derived cell lines commonly used to study IFN-stimulated genes (ISGs) that are responsible for establishing antiviral states *in vitro* (3,49). Previous studies have pointed to differences between the antiviral state induced by type I IFN in neuronal and non-neuronal cell lines (52). In order to empirically test this hypothesis NB41A3, NIH/3T3, and L929 cells were pretreated with IFN-β or vehicle alone and infected with VSV.

Analysis of viral titers by plaque assay showed that IFN-β worked effectively to inhibit VSV infections of all three cell types (Fig. 1A). However, Western blot analysis of cellular lysates harvested from the same cells showed a compelling difference between the neuronal and non-neuronal cell lines (Fig. 1B). The most prominent difference was seen with IFN-β pretreatment of these cells. NB41A3 cells induced by IFN-β led to a threefold reduction of VSV proteins, while similar treatment of NIH/3T3 and L929 cells yielded undetectable viral protein levels. After normalizing VSV protein signals with the GAPDH signal from each lane, it became apparent that viral infections of NB41A3 and L929 cells yielded similar VSV protein levels. VSV infections of NIH/3T3 cells, however, seemed to yield less viral proteins in their cellular lysates than either NB41A3 or L929 cells.

A type I IFN response in NB41A3 neuroblastomas does not alter VSV M protein ubiquitination

Mono-ubiquitination of VSV M is strongly associated with effective assembly and budding of virions (33,34). In order to test whether a type I IFN response alters M ubiquitination, NB41A3 cells were pretreated with IFN-β or vehicle alone, radiolabeled with ^{35}S-cysteine/methionine, and infected with VSV. NB41A3 cell lysates were subsequently analyzed via "double" immunoprecipitation. Cell lysates were first immunoprecipitated with both polyclonal anti-VSV antiserum and polyclonal anti-GAPDH antibodies to enrich for GAPDH and VSV proteins. Following dilution with buffer to nullify the effects of SDS, enriched protein solutions were again immunoprecipitated with polyclonal anti-GAPDH antibodies; however, in place of the polyclonal anti-VSV antiserum we used polyclonal anti-ubiquitin antibodies.

After resolving via SDS-PAGE, the levels of GAPDH were used as an internal normalizing factor to assess VSV M protein levels in the initial anti-VSV/anti-GAPDH immunoprecipitations. Those normalized M protein levels were then compared to those from the "double" immunoprecipitated anti-ubiquitin/anti-GAPDH samples. In this way changes in overall VSV M protein levels were compared to anti-ubiquitin-recognized VSV M protein levels (Fig. 2). The resulting statistical analysis showed no relevant change in ubiquitinated VSV M protein levels when compared to overall VSV M protein levels from IFN-β-treated neuroblastomas.

VSV P is hypophosphorylated in the cell lysates of neuroblastomas pretreated with IFN-β, but appears unchanged in VSV virions

Changes in P protein phosphorylation are critical for its function as a cofactor in RDRP modulation, and have been proven to be indispensable to VSV growth kinetics in an RDRP-independent fashion (8). To assess possible type I IFN-induced changes in viral protein post-translational modifications, we examined the phosphorylation of the P protein in neuroblastomas pretreated with IFN-β or vehicle alone. The level of P phosphorylation in cell lysates was first examined by immunoprecipitation of ^{32}P-orthophosphate-labeled lysates with an anti-P antiserum, followed by SDS-PAGE and autoradiography. When compared to untreated control cells, these experiments showed substantially decreased incorporation of ^{32}P-orthophosphate label into P protein isolated from infected, IFN-β-pretreated NB41A3 cells (Fig. 3A). These results were similar to those of experiments done with L929 and NIH/3T3 control cells (data not shown).

In order to differentiate between apparent changes due to phosphorylation or simply the presence of less overall protein, P protein was further purified by SDS-PAGE. For these experiments dual labeling, with ^{32}P-orthophosphate and ^{35}S-cysteine/methionine, was employed as both an indicator of protein phosphorylation and a control for viral protein levels, respectively. After purification by electrophoresis, those bands corresponding to VSV P protein and background bands were excised, dissolved, mixed with scintillation fluid, and analyzed by scintillation counter. The ratios of ^{35}S-associated counts to ^{32}P-associated counts were then compared between treatment groups. The effects of separate or dual labeling with these metabolic sources alone were assessed, by viral plaque assay, to neither have an effect on VSV production, nor to cause a change in VSV susceptibility to IFN-β inhibition in these cells (data not shown).

A 96.8% increase ($p = 0.003$) in the ratio of ^{35}S:^{32}P was observed in P protein isolated from IFN-β-treated VSV-infected neuroblastomas (Fig. 3B). These data, when combined with the moderate decrease in viral protein levels

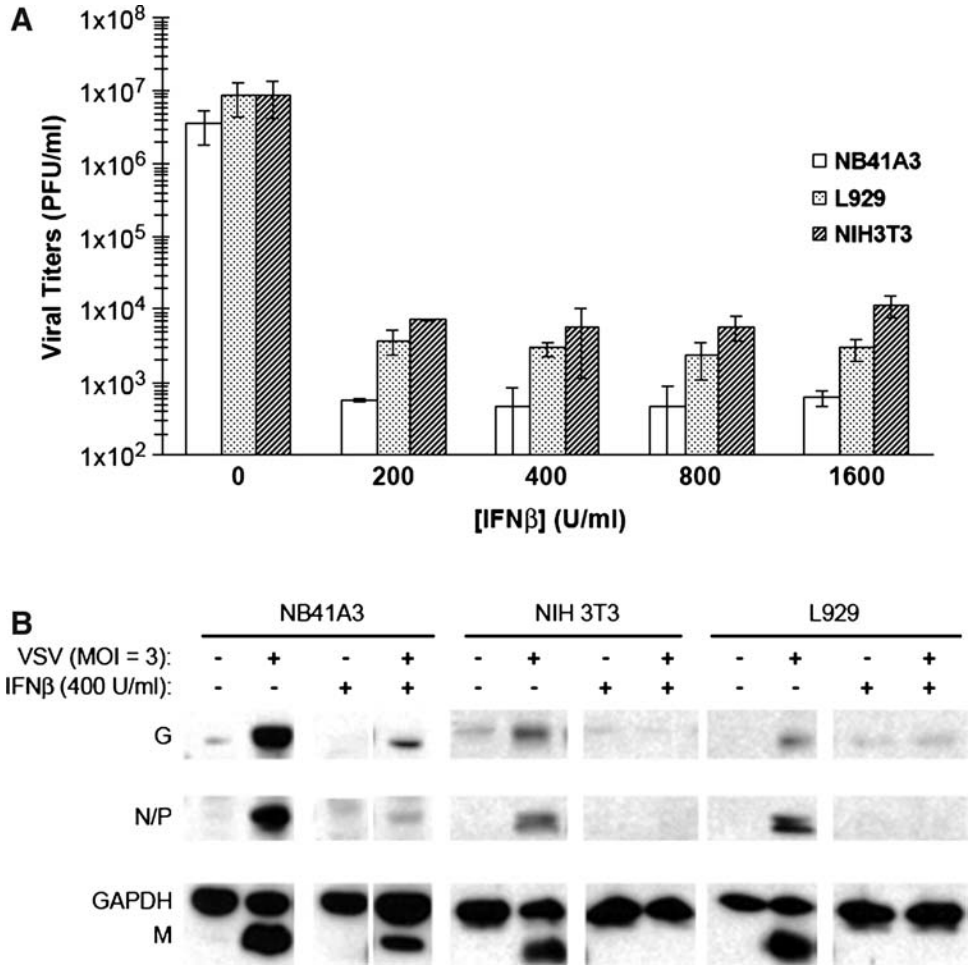

FIG. 1. IFN-β treatment suppressed both viral gene expression and infectious particle release in L929 and NIH/3T3 cells, but only partially inhibited such expression in NB41A3 cells. NB41A3, NIH/3T3, and L929 cells were treated for 24 h with a titration of IFN-β (200–1600 U/mL) or vehicle alone and infected with VSV (MOI = 3). At 6 hpi, cell supernatants and lysates were harvested. (**A**) Viral plaque assay. Supernatants were clarified via centrifugation at 200 RCF for 10 min, and viral titers assessed by plaque assay. Plaque assays revealed that all cell lines displayed a 10,000-fold reduction in VSV viral titers resulting from IFN-β pretreatment; error bars represent 2×the standard deviations from experiments done in triplicate. (**B**) Western blot analysis. Protein concentrations from cell lysates were normalized by Lowry assay (5 μg protein per lane), resolved via 12% SDS-PAGE, transferred to nitrocellulose, and probed with anti-VSV antiserum and anti-GAPDH polyclonal antibodies. While a threefold reduction in VSV viral proteins is observed in IFN-β-pretreated NB41A3 neuroblastomas, there are undetectable levels of VSV viral proteins in IFN-β-pretreated NIH/3T3 and L929 cell lysates. Figure representative of three replicate experiments.

found under the same experimental conditions, were interpreted as a decrease in the level of phosphorylation in those samples. When similar experiments were conducted with IFN-β-treated fibroblast-derived L929 and NIH/3T3 cells, no change in the ^{35}S:^{32}P ratio could be determined, consistent with undetectable P protein levels and a shutdown in protein synthesis (Fig. 3C and D).

To determine whether changes in VSV P phosphorylation carried over into proteins incorporated into released virions, supernatants were collected from IFN-β- or vehicle-treated, dual-labeled, VSV-infected NB41A3 cells. After ultracentrifugation, washing, and virion lysis, each viral lysate was also subjected to SDS-PAGE purification (Fig. 4A). Bands corresponding to virion-associated P protein were again excised, dissolved, and mixed with scintillation fluid; ^{35}S:^{32}P ratios were subsequently determined as described above. This revealed no significant difference ($p = 0.101$) in the phosphorylation of virion-associated P (Fig. 4B). We interpreted these data to indicate that there are populations of differentially phosphorylated P proteins within host cells, with the "properly" phosphorylated P population preferentially incorporated into released virus. Similar experiments with NIH/3T3 and L929 cells again yielded undetectable virion-associated P protein levels (Fig. 4C and D), a result consistent with both the absence of intracellular viral protein levels and low viral titers released from these cells (Fig. 1).

To extend and verify our experimental observations, experiments were performed to determine whether the anti-P antiserum recognized the entire P protein population. If the anti-P antiserum employed did not recognize the whole P population, different forms of P phosphorylation might exist that electrostatically block available P epitopes; such a

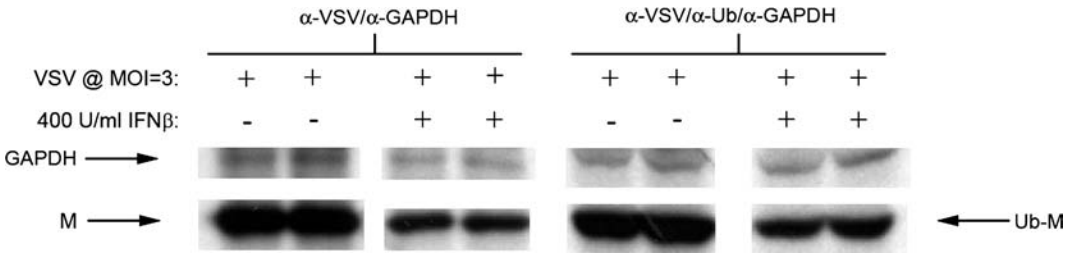

FIG. 2. An IFN-β-elicited antiviral state in NB41A3 neuroblastomas does not interfere with the mono-ubiquitination of the VSV M protein. Neuroblastomas treated for 24 h with 400 U/mL IFN-β or vehicle alone were infected with VSV (MOI = 3), then metabolically labeled with ^{35}S-cysteine/methione (100 μCi/mL). At 6 hpi, cell lysates were harvested and immunoprecipitated with anti-VSV antiserum and anti-GAPDH polyclonal antibodies. Following denaturation in 30 μL PBS + 1% SDS at 100°C, and dilution in 300 μL RIP buffer (to dilute out SDS effects), another immunoprecipitation was performed on these samples, with anti-ubiquitin and anti-GAPDH polyclonal antibodies. Samples were then resolved via 14% SDS-PAGE, dehydrated, infiltrated with 2,5-diphenyloxazole, dried, and exposed to film. Densitometric analysis of GAPDH-normalized samples revealed no significant difference between the levels of anti-ubiquitin-recognized VSV M protein from mock- and IFN-β-treated NB41A3 cells. Figure representative of three replicate experiments.

situation would potentially invalidate our observations of hypophosphorylation as mere artifact. Consequently, sequential immunoprecipitations were performed on cell lysates derived from VSV-infected NB41A3 cells, either treated with IFN-β or vehicle alone. In this experiment, cell lysates underwent successive immunoprecipitations with anti-P antiserum, followed by a final immunoprecipitation with an anti-VSV antiserum known to recognize all available epitopes for each viral protein (40). The resulting experiment did indeed demonstrate that the anti-P antiserum recognized the entire P-protein population from both untreated and IFN-β-treated neuroblastomas (Fig. 5).

VSV M is hyperphosphorylated in both cell lysates and viral particles derived from IFN-β-pretreated neuroblastomas

Experimental evidence has identified two major VSV M *in-vivo* phosphorylation sites with unknown function: a site N-terminal to Lys 19 (Ser 2, Ser 3, or Ser 17), and either Thr 31 or Ser 32 (35). Given the observed change in cellular P-protein phosphorylation found within IFN-β-treated neuroblastomas, we next investigated whether IFN-β treatment also affected M-protein phosphorylation. Dual-labeled, VSV-infected NB41A3 cell lysates derived from cells treated with IFN-β or vehicle alone were immunoprecipitated with an anti-VSV antiserum and subjected to SDS-PAGE. The resolved bands that corresponded to both VSV M and background were processed as described previously for the P protein. Relative to untreated controls, analysis of ^{35}S and ^{32}P counts in IFN-treated neuroblastoma lysates revealed a 73.2% ($p = 0.0024$) decrease in the M-protein ^{35}S:^{32}P ratio (Fig. 6A). Since this analysis was based upon normalized protein levels, we interpreted this change to indicate an increase in ^{32}P-orthophosphate incorporation, an indication of M hyperphosphorylation.

To determine if type I IFN treatment also altered M phosphorylation within virions, experiments were again conducted as those previously described for virion-associated P protein. The resulting analysis revealed that virion incorporated M protein, from viral infections of IFN-β-treated NB41A3 cells, was also hyperphosphorylated, as indicated by a 91% decrease ($p = 0.0005$) in the ^{35}S:^{32}P ratio relative to infected, mock-treated NB41A3 cells (Fig. 6B). Similar experimentation with the lysates and supernatants from IFN-treated NIH/3T3 and L929 cells yielded undetectable levels of both intracellular and virion-associated M protein (Fig. 6C and D). Although the lack of M protein from IFN-β-treated NIH/3T3 and L929 cells prevented comparison with protein isolated from NB41A3 cells, these data highlight the stark difference in the type I IFN-induced responses between these cell lines.

Shifts in isoelectric points for VSV viral proteins are consistent with IFN-β-induced changes in post-translational modifications

The observations made through analyzing variations in ^{35}S-cysteine/methionine and ^{32}P-orthophosphate incorporation in neuronal cells were consistent with IFN-β-induced alterations in M and P protein phosphorylation levels. If such findings were accurate, these varying levels of acidic moieties should be associated with corresponding changes in the charge-to-mass ratio of each protein. It has been well documented that, all things being equal, the addition of phosphate groups will shift a protein's isoelectric point (pI) towards the acidic direction of a pH gradient, while the removal of such groups will cause a more alkaline shift to occur. To that end, we sought to investigate whether changes in viral protein pI could be attributed to IFN-β, by examining these proteins via two-dimensional (2D) gel electrophoresis.

VSV-infected, ^{35}S-cysteine/methionine-labeled NB41A3 cell lysates derived from cells treated with IFN-β or vehicle alone, were immunoprecipitated with an anti-VSV antiserum. However, in place of using the standard SDS-PAGE sample buffer, a milder denaturing isoelectric focusing (IEF) sample buffer was employed to release viral proteins from their antigen-antibody complexes. The samples were subsequently normalized by ^{35}S-counts and resolved via IEF on a pH 3–10 ampholyte gradient. Afterwards, each IEF was further resolved by 14% SDS-PAGE and the resulting autoradiographs were analyzed using densitometry.

Under mock-treated conditions, VSV P protein appeared to resolve into two partially overlapping populations around pH 5 (Fig. 7A), consistent with the predicted pI from the P-protein primary sequence. Furthermore, the existence of two

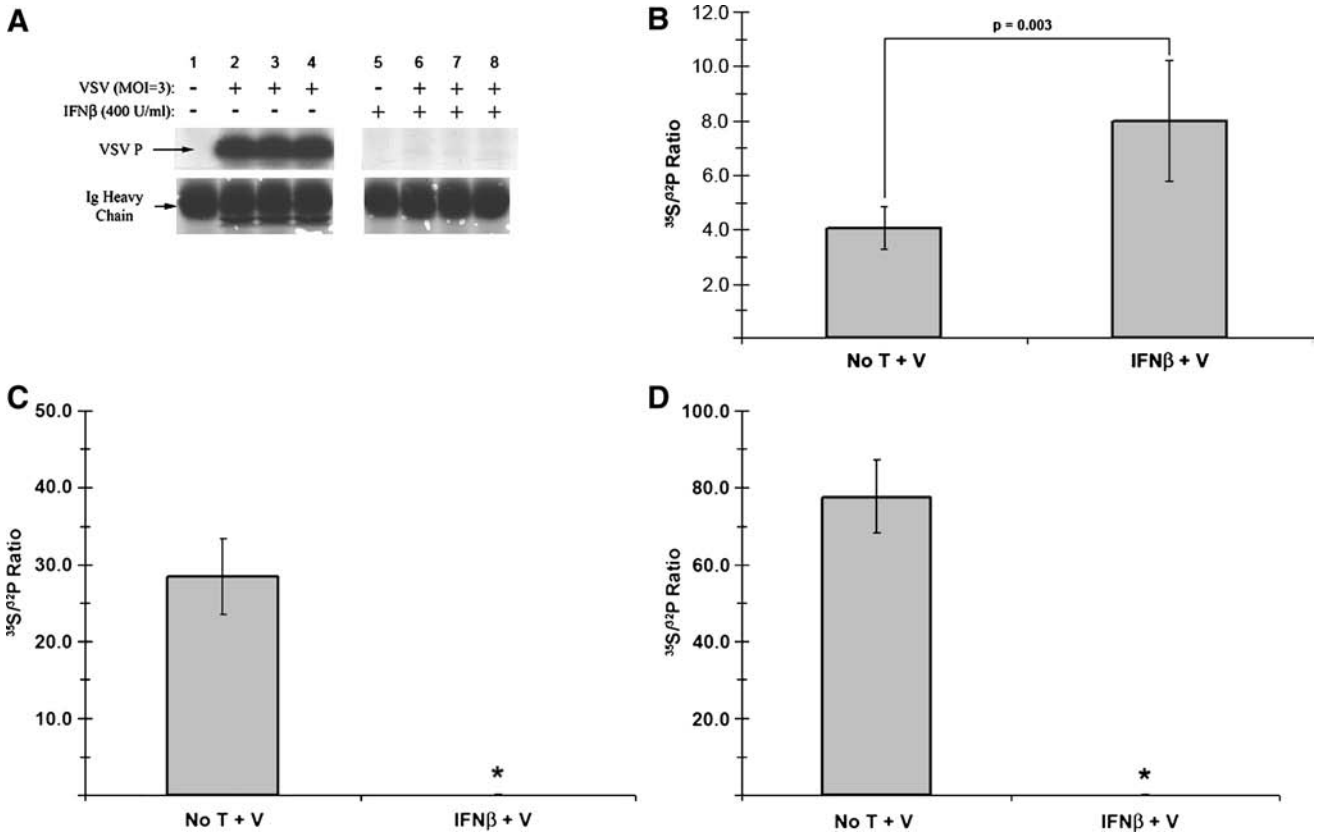

FIG. 3. VSV P protein phosphorylation is altered in neuronal cell lysates, but not virions from IFN-β-treated cells. Neuroblastomas treated for 24 h with 400 U/mL IFN-β or vehicle alone were infected with VSV (MOI = 3), then either labeled with ^{32}P-orthophosphate (50 μCi/mL), or dual-labeled with ^{32}P-orthophosphate (50 μCi/mL) and ^{35}S-cysteine/methione (100 μCi/mL). At 6 hpi, cell lysates were harvested and immunoprecipitated with anti-VSV P antiserum. Samples were then resolved via 12% SDS-PAGE, stained via Coomassie Brilliant Blue, and exposed to film. (**A**) Example of a typical autoradiograph from anti-VSV P immunoprecipitated ^{32}P-labled cell lysates, along with Coomassie-stained IgG heavy chain as a loading control. Lane 1 represents viral proteins from untreated, uninfected cells; lanes 2–4 represent viral proteins from untreated, VSV-infected samples from independent experiments; lane 5 represents viral proteins from IFN-β-treated, uninfected cells; lanes 6–8 represent viral proteins from IFN-β-treated, VSV-infected samples from independent experiments. (**B**) Analysis of ^{32}P and ^{35}S metabolically incorporated into P protein from dual-labeled cell lysates. Using the autoradiograph as a guide, bands corresponding to the VSV P protein were excised, dissolved in 30% H_2O_2, and added to scintillation fluid (1:6) for counting. The normalized ratio of ^{35}S-associated counts (representing total protein) to ^{32}P-associated counts (representing phosphorylated amino acids; ^{35}S:^{32}P) from purified P protein increased in neuronal lysates derived from IFN-β-pretreated cells, representative of hypophosphorylation. Analogous experiments carried out in (**C**) NIH/3T3 and (**D**) L929 cells were unable to assess any potential changes in ^{35}S:^{32}P, due to a complete shutdown in protein synthesis resulting from an IFN-β-established antiviral state in these cells (denoted by asterisks). Error bars correspond to 95% CI and the p-values were calculated based on Satterthwaite's method for calculating t-values from independent samples of unequal variances (n = 12) (No T + V, no treatment + virus; IFN-β + V, IFN-β + virus).

P-protein populations could be representative of both the transcription- and replication-competent protein forms. However, when P protein isolated from neuroblastomas treated with type I IFN was analyzed, the protein population became more diffuse, with an alkaline shift in position (Fig. 7A and B). These data were consistent with our previous data, which suggested P-protein hypophosphorylation in IFN-β-pretreated neuroblastomas, relative to mock-treated control samples (Fig. 4A).

A similar experiment to examine M protein from neuroblastoma cell lysates revealed a major protein population between pH 9 and 10, again consistent with the predicted pI for the M-protein primary sequence, with a tailing region extending towards mid-range pH values (Fig. 7A). Interestingly, M protein isolated from IFN-β-pretreated neuroblastomas, as analyzed by 2D gel electrophoresis, did not demonstrate any pronounced shift in pI (Fig. 7A and C). Instead we observed the loss of a major peak in the M-protein population when comparing 2D gels, of similar band intensities, from IFN-β-pretreated and mock-treated VSV-infected neuroblastomas. Additionally, since the VSV M protein is highly basic, the resolving power at the extreme ends of the pH gradient could have been insensitive to the effects of changes in phosphorylation levels.

As a side note, using an anti-VSV antiserum that recognized epitopes on all VSV proteins allowed a shift in the isoelectric focusing of the glycoprotein (G) population to be observed. In mock-treated, VSV-infected NB41A3 cell lysates

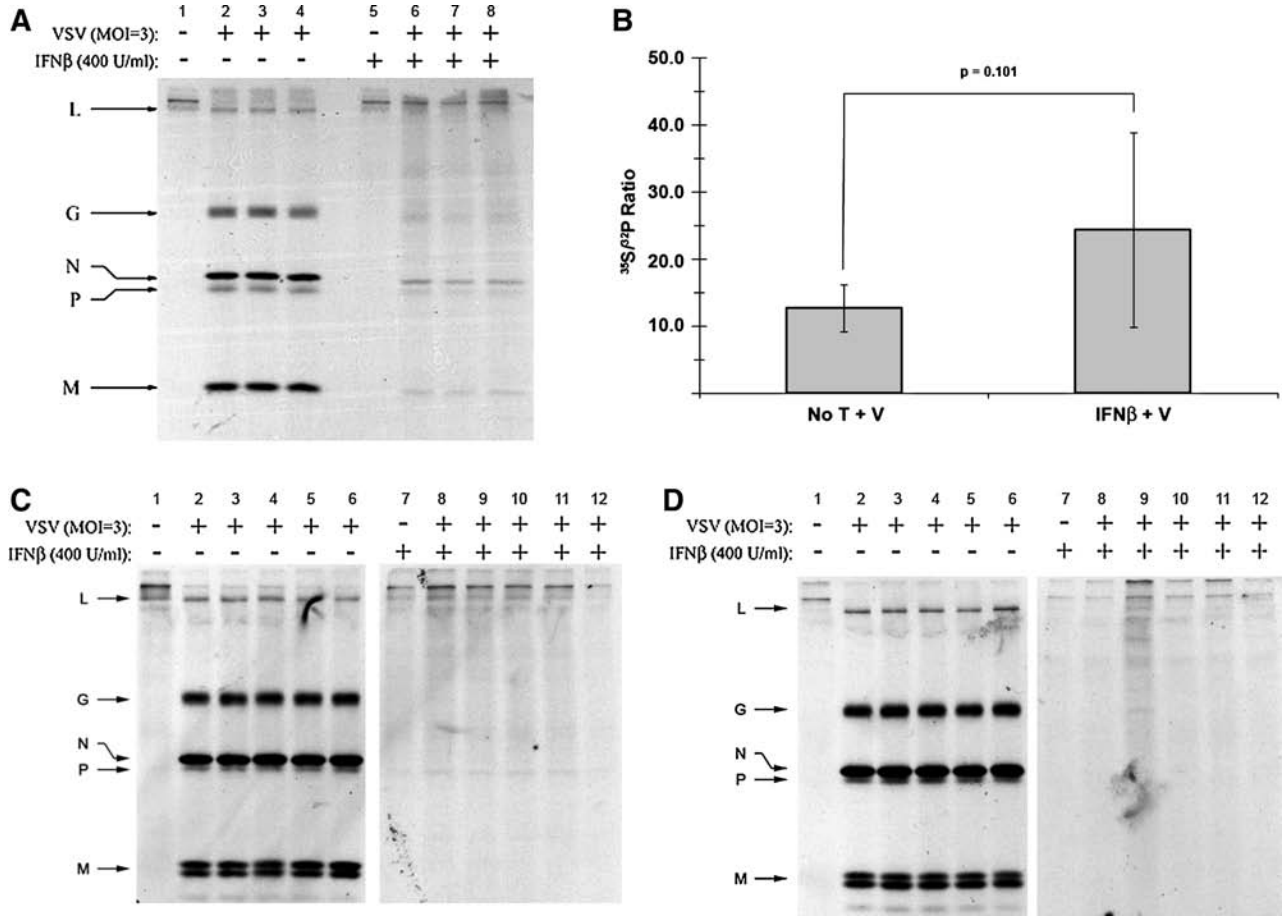

FIG. 4. VSV P protein phosphorylation is unchanged in viral particles recovered from IFN-β-pretreated cells. (**A**) Autoradiograph following SDS-PAGE of viral lysates. Neuroblastomas metabolically labeled as described in Fig. 3 were infected with VSV (MOI = 3), and viral supernatants were collected at 10 hpi. After removing cell debris via centrifugation (200 RCF for 10 min), VSV virions were subsequently pelleted via ultracentrifugation ($\sim$302,000 RCF for 15 min), washed with PBS, repelleted, and lysed. Viral lysates were resolved via 12% SDS-PAGE, stained with Coomassie Brilliant Blue, and exposed to film. Lane 1 represents viral lysates from untreated, uninfected NB41A3 cells. Lanes 2–4 represent viral lysates from untreated, VSV-infected NB41A3 cells from independent experiments. Lane 5 represents viral lysates from IFN-β treated, uninfected NB41A3 cells. Lanes 6–8 represent viral lysates from IFN-β-treated, VSV-infected NB41A3 cells from independent experiments. (**B**) Analysis of ^{32}P and ^{35}S metabolically incorporated into P protein from virions. Using the resulting autoradiographs as a guide, bands corresponding to virion-associated P protein were processed as describe in Fig. 3 for scintillation counting and ^{35}S:^{32}P ratio determination. Upon statistical analysis no change in the ^{35}S:^{32}P ratio of virion-associated P protein was observed in viral supernatants derived from IFN-β-pretreated NB41A3 cells (No T + V, no treatment + virus; IFN-β + V, IFN-β + virus). Analogous experimentation could not be performed with the viral supernatants obtained from (**C**) NIH/3T3 and (**D**) L929 non-neuronal control cells due to undetectable levels of virion-associated proteins. Lane 1 represents viral lysates from untreated, uninfected cells. Lanes 2–6 represent viral lysates from untreated, VSV-infected cells from independent experiments. Lane 7 represents viral lysates from IFN-β-treated, uninfected cells. Lanes 8–12 represent viral lysates from IFN-β-treated, VSV-infected cells from independent experiments. Error bars correspond to 95% CI and p-values were calculated based on Satterthwaite's method for calculating t-values from independent samples of unequal variances (n = 12).

the G protein focused into two broad acidic populations around pH 3–5 (Fig. 7A and D). However, in cellular lysates from IFN-β-treated, virally-infected NB41A3 cells, these two protein populations seemed to condense into one broad acidic population centered around pH 3.

Analogous experiments were also conducted with viral lysates from mock- and IFN-β-treated NB41A3 cells. Analysis of virion-associated VSV P protein, harvested from untreated NB41A3 cells, revealed a P-protein population focusing around pH 5 (Fig. 8A and B), the same region found in the cell lysates. Virion-associated VSV P protein from IFN-β-treated NB41A3 cells was dispersed into more acidic and basic populations that flanked the P-protein population identified in particles harvested from untreated cells (Fig. 8A and B). This dispersion pattern could be responsible for the highly scattered ^{35}S:^{32}P ratios observed (Fig. 4B), which we interpreted as background level variation in virion-associated P-protein phosphorylation patterns.

Next we turned our attention to VSV M isoelectric changes found in virions harvested from IFN-β-treated NB41A3 cells.

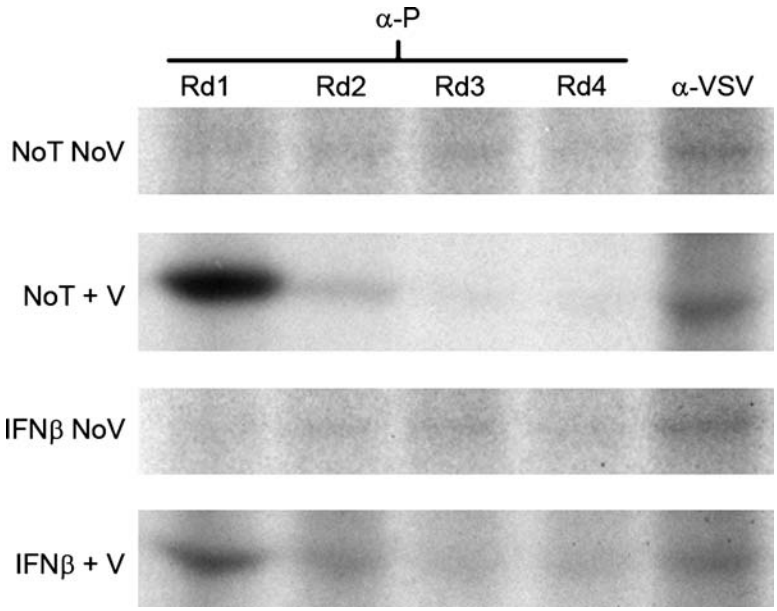

FIG. 5. The anti-VSV P antiserum used in biochemical analyses recognizes all P-protein populations. To rule out the possibility that the observed hypophosphorylation is an artifact generated by an inability of the anti-P antiserum to recognize all available epitopes within the P-protein population, sequential immunoprecipitations was performed. Briefly, anti-P antiserum was added to ^{35}S-cysteine/methionine-radiolabeled neuroblastomal lysates from NB41A3 cells treated with IFN-β or vehicle alone. After 24 h, the antigen-antibody complexes were precipitated out of solution using Pansorbin A, taking care to collect the original lysate for subsequent rounds of treatment with anti-P antiserum. After four rounds the original lysate was then treated with an anti-VSV antiserum known to recognize all viral epitopes. The resulting samples were resolved via 12% SDS-PAGE, dehydrated, infiltrated with 2,5-diphenyloxazole, dried, and exposed to film. The anti-P antiserum was able to recognize all epitopes corresponding to the P-protein population in both untreated and IFN-β pretreated NB41A3 cell lysates (No T No V, no treatment, no virus; No T + V, no treatment + virus; IFN-β No V, IFN-β, no virus; IFN-β + V, IFN-β + virus).

As demonstrated in cell lysates (Fig. 7A and C), VSV M protein focused at the extreme basic end of the ampholyte gradient, representing a pH between 9 and 10. The isoelectric focusing pattern for virion-associated M protein harvested from IFN-β-treated neuronal cells exhibited a more acidically diffuse pattern with a lone population reaching into the pH 4–5 range (Fig. 8A and C). We interpreted these data as corroborating our findings of hyperphosphorylated virion-associated M protein, by ^{35}S:^{32}P ratios (Fig. 6B), in particles budded from IFN-β-treated NB41A3 cells.

Lastly, IFN-β-induced changes in virion-associated G protein pI were observed in patterns similar to those found in neuroblastoma cell lysates (Fig. 8A and D). These data gave credence to type I IFN-induced changes in G protein glycosylation. However, the extent and functional relevance of those changes as they pertain to reduced infectious viral titers remains to be determined.

IFN-β-induced VSV M hyperphosphorylation leads to changes in its protein-protein interactions

While P protein hypophosphorylation may alter viral RNA-dependent RNA polymerase (RDRP) function, it is difficult to imagine such changes having an effect on viral assembly. However, changes in M-protein post-translational modification could potentially have direct implications on the assembly and budding process. To test our hypothesis that a component of type I IFN-mediated actions in neurons compromises VSV assembly, we examined whether M-protein hyperphosphorylation resulted in aberrant ratios of VSV proteins incorporated into released particles.

Viral lysates from purified virions were normalized by ^{35}S counts, resolved via SDS-PAGE, and the resulting autoradiographs were analyzed using densitometry (Fig. 9A). In virus derived from IFN-β-treated cells, a 26% increase ($p = 0.002$) in the nucleocapsid (N)-to-M ratio was observed as the only significant difference between treatment groups. Such an increase in the N:M protein ratio, found in virions released from IFN-β-treated neuroblastomas, could have been caused by diminished avidity between the interactions of these two proteins resulting from M hyperphosphorylation.

To test whether IFN-β-induced M protein hyperphosphorylation had an effect on N and M protein-protein interactions, ^{35}S-radiolabeled, VSV-infected NB41A3 cell lysates, from cells treated with IFN-β or medium alone, were immunoprecipitated with an anti-VSV M-specific monoclonal antibody (38) and resolved via SDS-PAGE. M protein from untreated, VSV-infected control lysates showed an inability to co-precipitate N protein. This inability of the M protein to pull down N also extended to IFN-β-treated NB41A3 lysates (Fig. 9B). We interpreted these data as indicating that the vast majority of M protein in VSV-infected cells, whether from mock- or IFN-β-treated neurons, was not associated with the ribonucleoprotein (RNP). The majority of M protein was likely bound to the nuclear pore complex (22,47), mitochondria (39), and the inner face of the plasma membrane, and/or free within the cytoplasm (5,6,44).

Conversely, when the reciprocal immunoprecipitation experiment was conducted using a polyclonal anti-N antiserum (25), M protein was successfully co-precipitated with N from mock-treated, VSV-infected control cell lysates (Fig. 9C). The ability of N protein to pull down M was much less effective in IFN-β-treated NB41A3 lysates. We interpreted these data as indicating that altered post-translation of VSV M protein (e.g., hyperphosphorylation) impaired its ability to interact with RNP complexes.

The discrepancy between co-immunoprecipitation experiments was further investigated by assessing the recognition of the anti-M monoclonal antibody towards M protein populations. Sequential immunoprecipitations, similar to those described for the anti-P antiserum, demonstrated that the anti-M monoclonal antibody (designated MAb 23H12; [38]) used in these experiments only recognized a fraction of the total M protein population in both IFN-β-treated and mock-treated,

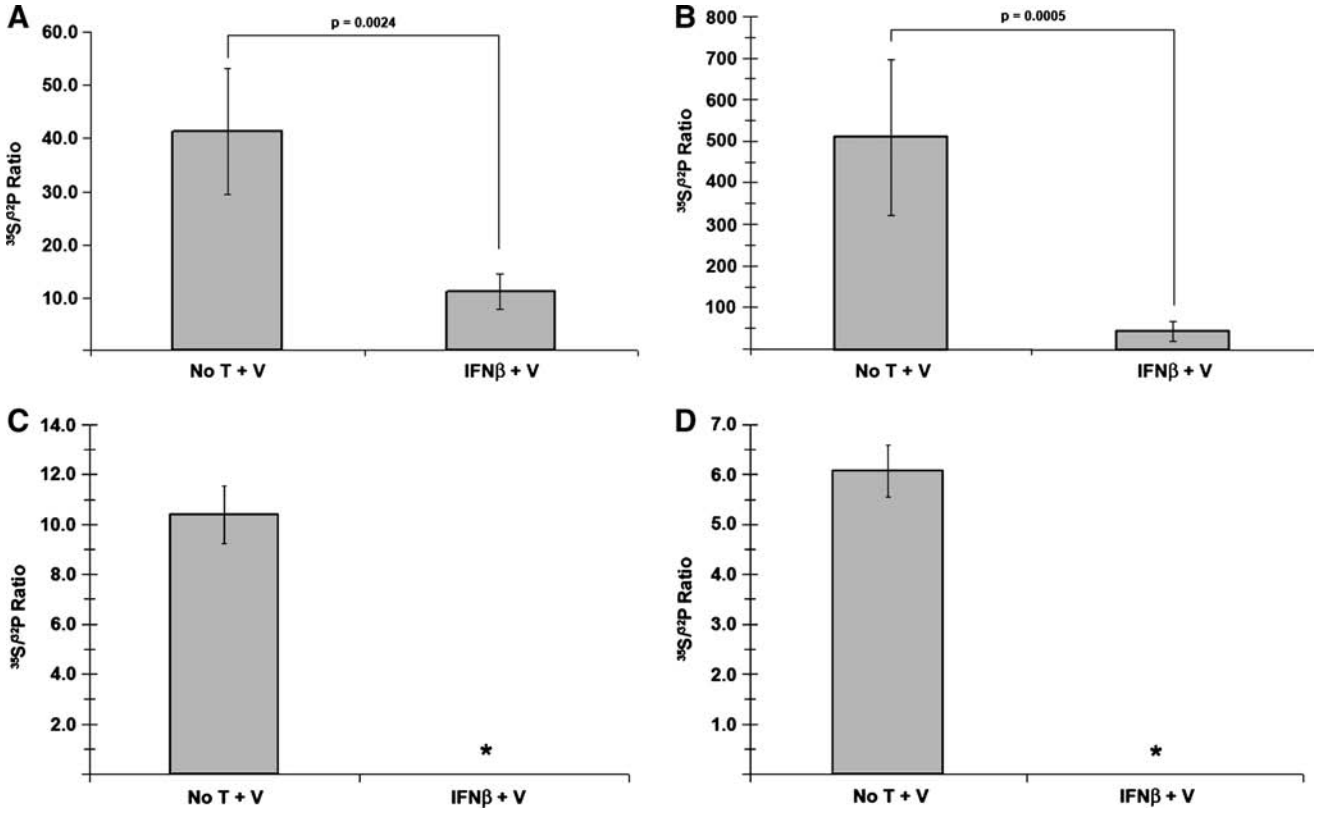

FIG. 6. VSV M protein is hyperphosphorylated in both neuronal cell lysates and virions derived from cells pretreated with IFN-β. (**A**) Analysis of ^{32}P and ^{35}S metabolically incorporated into M protein from dual-labeled cell lysates. As previously described in Fig. 3, neuroblastomas were treated with 400 U/mL IFN-β or vehicle alone, infected with VSV (MOI = 3), and dual-labeled with ^{32}P-orthophosphate (50 μCi/mL) and ^{35}S-cysteine/methione (100 μCi/mL). Cell lysates were subsequently immunoprecipitated with anti-VSV antiserum (at 6 hpi), resolved via 12% SDS-PAGE, stained with Coomassie Brilliant Blue, and exposed to film. Bands corresponding to VSV M protein were excised, using the developed film as a guide, dissolved in 30% H_2O_2, and added to scintillation fluid (1:6) for counting. The ^{35}S:^{32}P ratio associated with the M protein decreased in neuronal lysates derived from IFN-β-pretreated cells, representative of hyperphosphorylation. (**B**) Analysis of ^{32}P and ^{35}S metabolically incorporated into M protein from virions. Viral supernatants were collected and viral lysates were prepared as described in Fig. 4. Viral lysates were then resolved via 12% SDS-PAGE, stained with Coomassie Brilliant Blue, and exposed to film. Bands corresponding to virion-associated M protein were excised, using the resulting autoradiograph as a guide, then dissolved in 30% H_2O_2, and added to scintillation fluid (1:6) for counting. The ^{35}S:^{32}P ratio from virion-associated M protein decreased in virus derived from IFN-β-pretreated cells, representative of the hyperphosphorylation observed within the cell lysates. Analogous experimentation could not be performed with (**C**) NIH/3T3 and (**D**) L929 cell lines, due to undetectable levels of VSV M in cell lysates (*) and the corresponding supernatants (*) (supernatant ^{35}S:^{32}P ratio data not shown). Error bars correspond to 95% CI and *p*-values were calculated based on Satterthwaite's method for calculating *t*-values from independent samples of unequal variances (n = 12) (No T + V, no treatment + virus; IFN-β + V, IFN-β + virus).

VSV-infected neuroblastoma cell lysates (Fig. 10A). The remaining populations of M protein that were not recognized by MAb 23H12 probably represented either conformationally different or alternately modified forms of the protein.

Western blot analysis of NB41A3 cells transiently transfected to express the M51R mutant M protein—a loss-of-function mutant of M no longer able to block host RNA export from the nucleus (17)—revealed that the single point mutation (changing a polar sulphydryl group to a charged residue) was sufficient to destroy the MAb 23H12 epitope (Fig. 10B). Considering this experiment was conducted under denaturing conditions, it seems logical that any MAb 23H12-unrecognized forms of the M protein would be due to protein modifications that chemically altered residues within the epitope, although direct evidence for this has yet to be shown. We interpret these data to indicate that phosphorylation sites within the M protein may interfere with its ability to form stable complexes with the viral RNP (through interactions with N); such a scenario would likely contribute to lowered efficiency of viral assembly and release in IFN-β-treated neuronal cells. Sequential immunoprecipitations with the anti-N antiserum showed that the entire N protein population was recognized in both mock- and IFN-β-treated groups (Fig. 10C).

Discussion

Our experiments demonstrate compelling evidence that type I IFN-elicited responses in neuronal cells differ profoundly from those responses seen in more traditionally used fibroblast-derived cell lines (e.g., NIH/3T3 and L929 cells). In

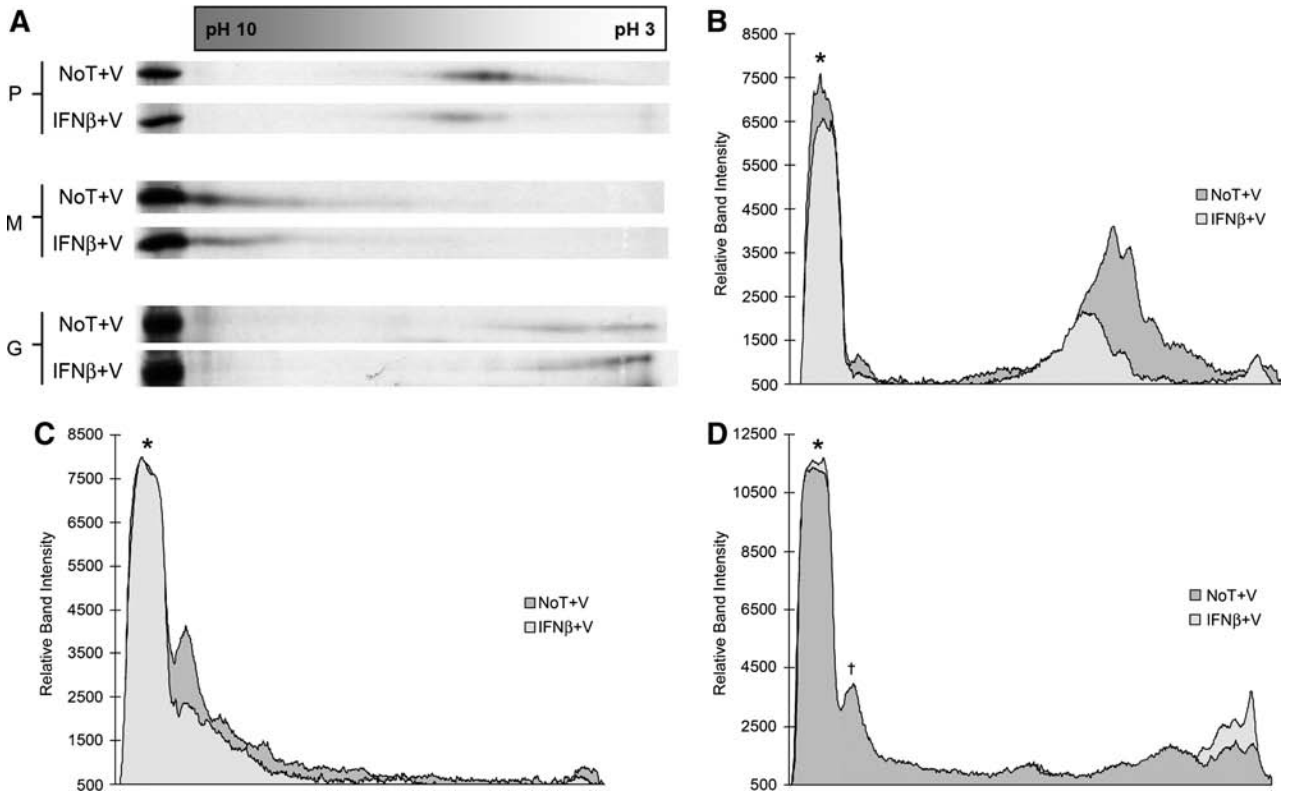

FIG. 7. Two-dimensional electrophoresis of VSV proteins from cell lysates demonstrates pI shifts consistent with hypo- and hyperphosphorylation. (**A**) Neuroblastomas treated with and without 400 U/mL IFN-β were infected with VSV (MOI = 3), then labeled with ^{35}S-cysteine/methionine (100 μCi/mL). Cell lysates were subsequently immunoprecipitated with anti-VSV antiserum (at 6 hpi), and resolved via isoelectric focusing on pH 3–10 ampholyte gradients. The resulting isoelectrically-focused samples were further resolved via 14% SDS-PAGE. These gels were then dehydrated in DMSO, infiltrated with 2,5-diphenyloxazole, dried, and exposed to film. The autoradiographs were then subjected to densitometric analysis using Un-Scan-It Gel software version 5.1. (**B**) A shift in the P-protein population towards a more basic distribution was observed in cell lysates isolated from IFN-β-pretreated neuroblastomas, compared to untreated control cells, consistent with hypophosphorylation. (**C**) A shift in the peak M-protein population towards a more diffuse acidic distribution was observed in cell lysates isolated from IFN-β-pretreated neuroblastomas, compared to untreated control cells, consistent with hyperphosphorylation. (**D**) The G protein from mock-treated NB41A3 cells focused into two broad acidic populations between pH 3 and 5. However, in cellular lysates from IFN-β-treated cells these two protein populations condense into one broad acidic population centered around pH 3. The asterisk represents each proteins control band for conventional SDS-PAGE. The dagger represents a background, nonviral protein that was verified by running the uninfected control samples (data not shown). Autoradiographs and densitometry results shown are representative of experiments done in triplicate (No T + V, no treatment + virus; IFN-β + V, IFN-β + virus).

each cell line used in this study pretreatment with IFN-β resulted in a >10,000-fold reduction in infectious VSV titers (Fig. 1A). While such a precipitous drop in viral titers was easily explained by undetectable viral protein levels in IFN-β-treated NIH/3T3 and L929 cell lines, invariably due to a cessation in host cell translation resulting from eIF2α phosphorylation by dsRNA-dependent protein kinase R, only a threefold reduction in viral protein expression was observed in similarly treated NB41A3 neuroblastomas (Fig. 1B). These results are in agreement with previously published data indicating a marginal decrease in VSV viral transcript and protein expression within type I IFN-treated neuroblastomas and primary neurons *ex vivo* (52).

This evidence led to the hypothesis that VSV assembly and release was inhibited through changes in viral protein post-translational modifications caused by a type I IFN-established antiviral state within neuronal cells, the most relevant post-translation modification pertaining to VSV assembly being M mono-ubiquitination. A well-known characteristic of enveloped viruses, which bud from the plasma membrane, is the occurrence of "late" domains. These "late" domains were first identified by mutational analysis that resulted in abrogation of viral infectious cycles at a "late stage," namely the budding process (18). Further studies later identified "late" domains (whose consensus sequences are PPXY, PT/SAP, and YXXL) as the targets for specific E3 ubiquitin ligases, as well as TSG101 and VPS4—integral components of the endosomal sorting complex for transport (ESCRT) machinery (48). The ESCRT pathway is currently believed to be hijacked by several enveloped viruses (e.g., VSV) in order to facilitate the budding process.

VSV M has been shown to become ubiquitinated in a PPPY-dependent manner (27). To test whether or not a type I IFN-established antiviral state would alter the ubiquitinated

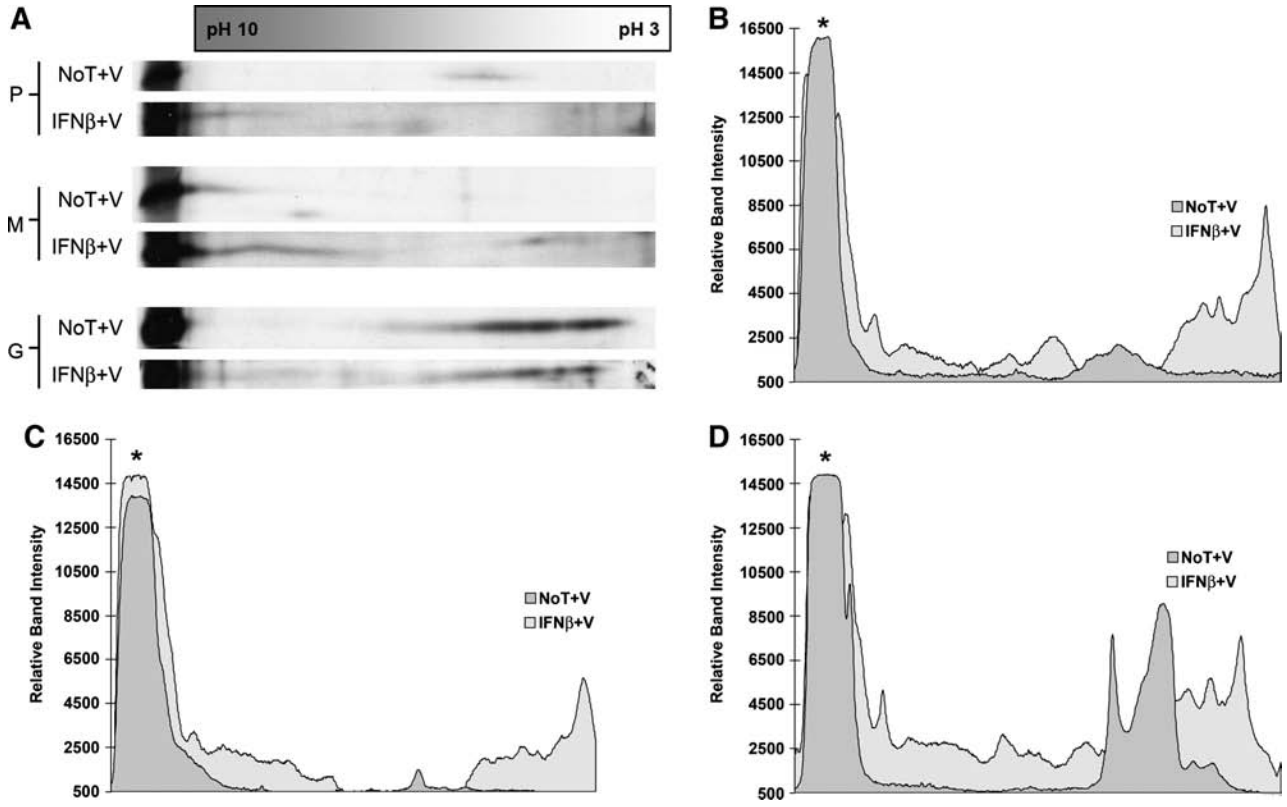

FIG. 8. Two-dimensional electrophoresis of VSV virion-associated proteins demonstrates an isoelectric point shift in M protein consistent with hyperphosphorylation. (**A**) Neuroblastomas treated with and without 400 U/mL IFN-β were infected with VSV (MOI = 3), then labeled with ^{35}S-cysteine/methionine (100 μCi/mL). Viral supernatants were collected 10 hpi and cell debris was removed by centrifugation. VSV virions were pelleted via ultracentrifugation ($\sim$302,000 RCF for 15 min), washed with PBS, repelleted, and lysed. Viral lysates were resolved via isoelectric focusing on pH 3–10 ampholyte gradients. The resulting isoelectrically focused samples were further resolved via 14% SDS-PAGE. The gels were then dehydrated in DMSO, infiltrated with 2,5-diphenyloxazole, dried, and exposed to film. The autoradiographs were then subjected to densitometric analysis using Un-Scan-It Gel software version 5.1. (**B**) Virion-associated P protein harvested from untreated NB41A3 cells focused into a single population around pH 5. Virion-associated P protein from IFN-β-treated NB41A3 cells, however, was dispersed into more acidic and basic populations. (**C**) A shift in the peak M protein population towards a more acidic distribution, as well as the identification of a lone protein population between pH 4–5, was observed in viral lysates isolated from IFN-β-pretreated neuroblastomas, compared to untreated control cells, consistent with hyperphosphorylation. (**D**) IFN-β-induced changes in virion-associated G protein pI were observed in patterns similar to those found in neuroblastoma cell lysates, namely two broad acidic populations between pH 3 and 5 in virions from untreated cells condensed into one broad acidic population centered around pH 3 in virions from IFN-β-pretreated neuroblastomas. The asterisk represents each proteins control band for conventional SDS-PAGE. The dagger represents a background, nonviral protein that was verified by running the uninfected control samples (data not shown). Autoradiographs and densitometry results are representative of experiments done in triplicate (No T + V, no treatment + virus; IFN-β + V, IFN-β + virus).

status of VSV M, we looked for any changes in the ratio of ubiquitinated M to GAPDH loading control through immunoprecipitations. Comparison of IFN-β-treated and mock-treated neuroblastomas revealed no significant difference in ubiquitinated M levels in cell lysates (Fig. 2).

We next turned our attention to another type of post-translational modification: phosphorylation. In addition to its critical role in modulating RDRP function (8,15), VSV P protein phosphorylation status has been shown to be crucial for bridging the gap between the N-RNA template and the large subunit (L) protein (4,19). In addition to its role as a modulator of RDRP activity, the VSV phosphoprotein (P) facilitates encapsidation of the viral genome by binding newly-formed N protein and forming an RNA-free N°-P complex (26,42), thereby acting as a necessary chaperone involved in nascent formation of the RNP core. The RNP is comprised of the negative-sense, single-stranded RNA viral genome encapsidated by the nucleocapsid (N) protein. N encapsidation effectively protects the viral genome by both obscuring double-stranded RNA replication intermediates from detection by the pattern recognition proteins host cells employ to identify pathogen-associated molecular patterns, and by protecting the viral genome from the functional RNases those proteins activate (20).

Thus, in theory, P-protein phosphorylation is vital to viral propagation, but phosphorylation has also been experimentally shown to be indispensable to VSV growth kinetics (8). BHK-21 cells infected with a VSV P227 mutant exhibited milder cytopathic effects and a reduction in apoptosis, much like what was observed with IFN-β-treated neuroblastomas (52). Likewise, it has been well documented that treatment with IFN-β effectively inhibits the infection of

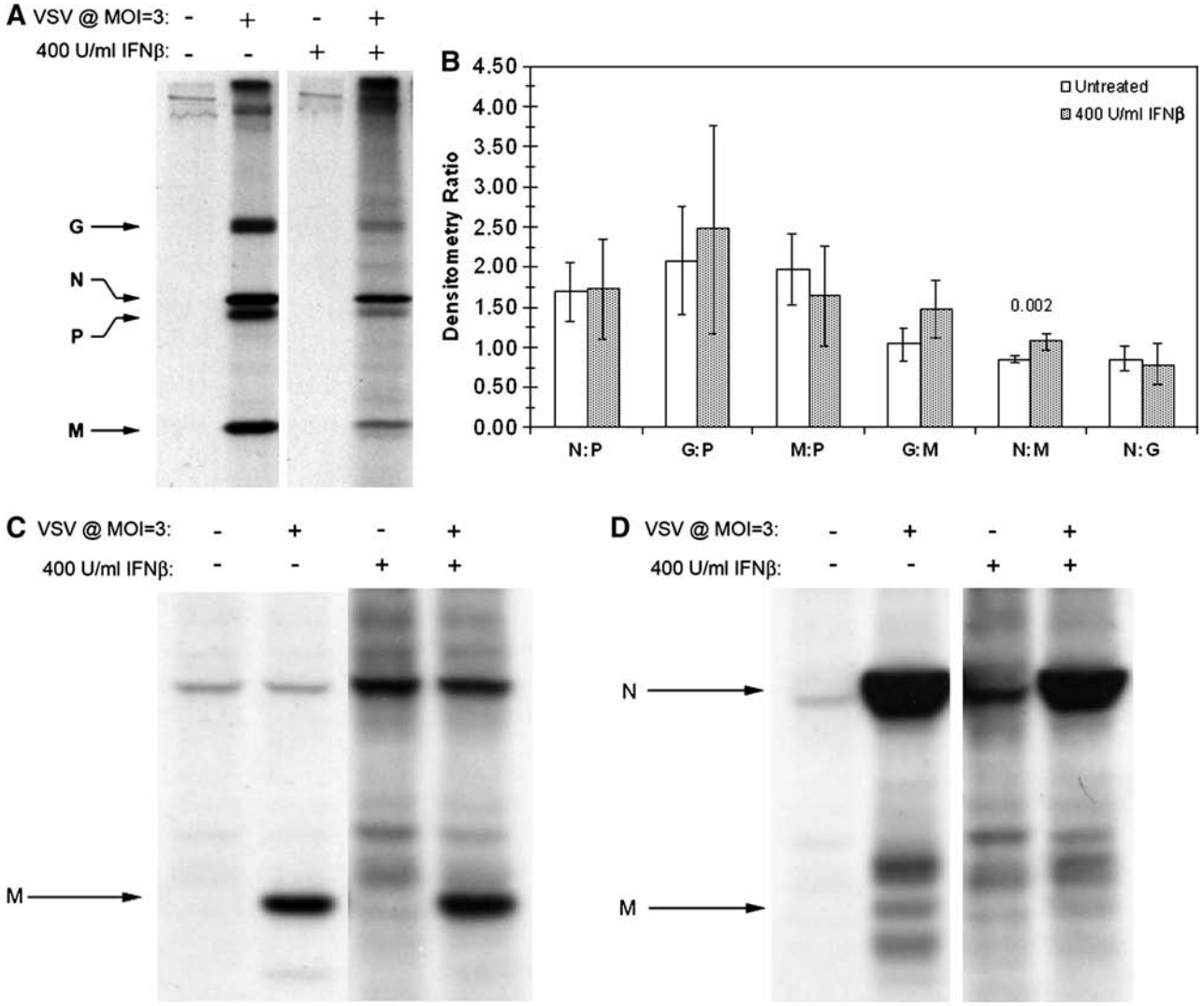

FIG. 9. Altered phosphorylation of VSV M affects interactions with VSV N in cells and virions. (**A**) Neuroblastomas treated with and without 400 U/mL IFN-β were infected with VSV (MOI = 3), then labeled with ^{35}S-cysteine/methionine (100 μCi/mL). Viral supernatants were collected 10 hpi and cell debris was moved by centrifugation. VSV virions were pelleted via ultracentrifugation (~302,000 RCF for 15 min), washed with PBS, repelleted, and lysed. The ^{35}S-labeled viral supernatants were then normalized using ^{35}S counts, and resolved via 12% SDS-PAGE. Subsequently the gels were dehydrated in DMSO, infiltrated with 2,5-diphenyloxazole, dried, and exposed to film. Autoradiographs of VSV viral lysates were then used to determine the ratios of virion-associated proteins via densitometric analysis using Un-Scan-It Gel software version 5.1. Statistical analysis revealed a difference between the ratio of virion-associated N and M proteins resulting from IFN-β pretreatment. Due to the nature of N and M interactions necessary for proper virion assembly, the difference in N:M ratio suggested a possible change in the affinity of these proteins for one another. Data represent the mean of three experiments with each experimental condition done in triplicate. Error bars correspond to 95% CI and the *p*-values were determined by Satterthwaite's method for calculating *t*-values from independent samples of unequal variances. (**B**) Immunoprecipitations of cell lysates (at 6 hpi) were conducted using the 23H12 monoclonal anti-VSV M antibody and resolved via 14% SDS-PAGE. Subsequently, the gels were dehydrated in DMSO, infiltrated with 2,5-diphenyloxazole, dried, and exposed to film. VSV M did not co-precipitate detectable N in either treatment group, a result most likely due to a preponderance of M protein either free within the cytosol or in non-RNP complexes. (**C**) Co-immunoprecipitations as described in B, using anti-VSV N antiserum revealed a change in the ability of N to co-immunoprecipitate M from IFN-β-treated neuronal lysates. Autoradiographs are representative of experiments done in triplicate.

IFN-sensitive viruses (e.g., VSV) in IFN-responsive cell lines (Fig. 1A). In this manner experiments were conducted to assess any changes in P-protein phosphorylation status that may have resulted from the establishment of a type I IFN antiviral state in neuronal cells, and to compare those changes (if any) with similar experiments done using non-neuronal cells.

Using immunoprecipitation coupled with SDS-PAGE purification, an IFN-β-induced 96.8% ($p = 0.003$) change in ^{32}P-orthophosphate incorporation, as well as an alkaline shift in P-protein isoelectric focusing were found, suggesting P-protein hypophosphorylation in the neuronal cell line NB41A3. Unfortunately, due to undetectable viral protein levels resulting from a type I IFN response in L929 and NIH/3T3 cells, no

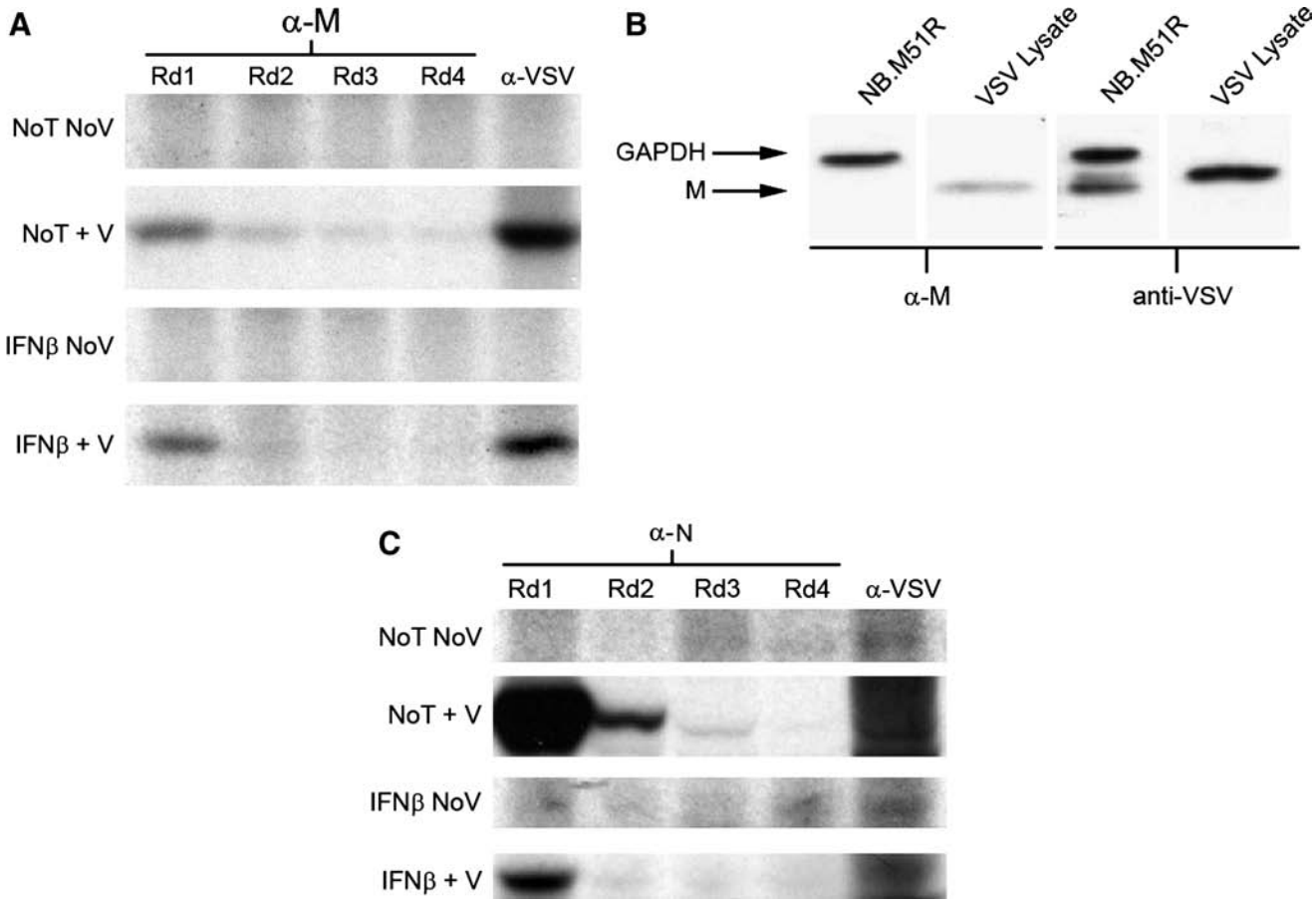

FIG. 10. Anti-M protein MAb binds to a portion of the M protein population in infected cell lysates. (**A**) Sequential immunoprecipitations were conducted, as described previously, using the 23H12 monoclonal anti-M antibody. The resulting data revealed an M-protein population not recognized by the anti-M monoclonal antibody, which may represent M protein whose epitope is obstructed by post-translational modifications or protein-protein interactions. (**B**) Western blot analysis of NB41A3 cells transiently transfected with 2 μg of a plasmid expressing the M51R loss-of-function mutant M protein. Analysis revealed that the single point mutation in M51R was sufficient to destroy M protein recognition by MAb 23H12. (**C**) Sequential immunoprecipitations were conducted, as previously described, using anti-VSV N antiserum. The anti-VSV N antiserum was able to recognize all epitopes corresponding to the N-protein population from both mock- and IFN-β-pretreated NB41A3 cell lysates. The autoradiographs and blot shown are representative of experiments done in triplicate (No T No V, no treatment, no virus; No T + V, no treatment + virus; IFN-β No V, IFN-β, no virus; IFN-β + V, IFN-β + virus).

assessment of P-protein phosphorylation could be made to determine whether the observations made in NB41A3 cells were specific or not to neuronal cell lines. While the inability to detect changes in ^{35}S:^{32}P ratios offered no insight into the general role of altered P-protein phosphorylation as a means of thwarting a VSV infection, it did highlight profound differences between neuronal and non-neuronal type I IFN-established antiviral states. Equally frustrating have been attempts to correlate the results shown here with primary neurons *ex vivo*. The number of cells needed to yield sufficient material for biochemical analysis using the techniques designed in this paper proved to be impractical with the current protocol for culturing primary neurons. To that end, efforts are ongoing to immortalize primary neurons using a truncated form of the SV40 large T antigen (53).

P-protein hypophosphorylation would lead one to predict reduced functionality in the viral RDRP. Experiments are also in progress to employ a well-documented RDRP functional assay to test such a hypothesis. However, the well-established method of using VSV N, P, and L proteins, along with a fragmented N reporter gene flanked by VSV promoters (56), utilizes a T7 promoter-driven system requiring initial infection with vaccinia virus. Efforts are also underway to substitute an alternative driver so that the effects of a type I IFN response on RDRP function can be studied free of other contaminating viral components.

Regardless of its effects on RDRP function, we next sought to determine if hypophosphorylated P protein was incorporated into budding virions. Implementing experiments analogous to those used to quantify changes in the P protein from cell lysates, we demonstrated that IFN-β treatment had no statistical impact on virion-associated P-protein phosphorylation (Fig. 4B). However, after 2D gel analysis, it seemed that the ability to assess changes in phosphorylation was complicated by a shift in the virion-associated P-protein population towards both a more basic focusing (indicative of hypophosphorylation), as well as a more acidic shift (Fig. 8A and B). This observed dichotomy in virion-associated P-protein isoelectric focusing no doubt led to the high p-value determined for the ^{35}S:^{32}P ratios found in IFN-β-treated

Table 1. VSV Matrix Primary Structural Analysis for Putative Phosphorylation Sites[a]

Matrix protein, Indiana, San Juan	M***S****S*LKKILGL KGKGKK***S***KKL GIAPPP***Y***EED ***T******S***MEYAPSAP IDKSYFGVDE 50 MD***T******Y***DPNQLR YEKFFF***T***VKM TVR***S***NRPFR***T*** ***Y***SDVAAAV***S***H WDHM***Y***IGMAG 100 KRPFYKILAF LGSSNLKATP AVLADQGQPE YHAHCEGRAY LPHRMGK***T***PP 150 MLNVPEHFRR PFNIGLYKGT IELTM***T***I***Y***DD E***S***LEAAPMIW DHFNSSKF***S***D 200 FREKALMFGL IVEKKASGAW VLDSIGHFK

[a]Underlined sequences denote viral late domains; bold and italicized amino acids represent putative phosphorylation sites based on NetPhospho 2.0 results, x-ray crystallography, and experimental data.

samples, leading us to determine that hypophosphorylated P protein was not convincingly incorporated into viral particles.

A reduction in RDRP activity would not fully explain the orders of magnitude of difference between viral transcript and protein expression, and the titers of infectious particles resulting from IFN-β-treated neuronal cells. Consequently, we turned our attention to the most likely candidate for disruption in viral assembly: the M protein. As stated before, experimental evidence has identified two major VSV M *in-vivo* phosphorylation sites centered around a site N-terminal to Lys 19 (Ser 2, Ser 3, or Ser 17), and either Thr 31 or Ser 32 (35). Mutational ablation of one or both of these sites had no effect on the ability of viruses bearing those mutations to bud, leading to uncertainty in the function attributed to these modifications.

Our experiments demonstrated a 73.2% ($p = 0.0024$) change in ^{32}P-orthophosphate incorporation, indicative of M protein hyperphosphorylation in IFN-β-treated NB41A3 cells only, since we were unable to be assess similar changes in L929 and NIH/3T3 cells due to undetectable M protein levels. Interestingly, 2D gel electrophoresis did not reveal a physical acidic shift in M-protein isoelectric focusing—as would be expected of hyperphosphorylation—but rather a cumulative shift due to the loss of a largely basic M protein population (Fig. 7A and C). We postulated that this counterintuitive isoelectric shift could be the result of impaired resolving power at the extreme ends of the pH gradient, effectively masking pronounced changes in M protein pI due to altered phosphorylation in such a highly basic protein. Yet another difference in our observations with altered M-protein phosphorylation was that intracellular hyperphosphorylation carried over into viral particles, with a representative acidic shift in M-protein isoelectric focusing (Fig. 8A and C).

VSV M is critically involved in mediating the budding process (5,6,33). Consequently, a type I IFN-induced cellular response in neurons that impairs VSV assembly via M-protein hyperphosphorylation should yield differences in viral protein levels within budded viral particles. Indeed, normalization and densitometric analysis of viral lysates (Fig. 9A) did reveal such a statistical difference in the levels of N with respect to M protein in virions recovered from IFN-β-treated neuroblastomas. Furthermore, this change in N and M protein levels was attributed to a change in N and M complex formation, as demonstrated by co-immunoprecipitation assay (Fig. 9C). A similar change in the affinity of M for N could only be inferred, since the monoclonal antibody (23H12) (38) we employed for that co-immunoprecipitation assay did not recognize the entire M-protein population (Fig. 10A).

Interestingly, it was further shown that 23H12 did not recognize M protein with a single point mutation (M51R) in a site known to interact with and inhibit the host mRNA export factor Rae1/mrnp41 (16). A complete disruption in the 23H12 epitope was most likely caused by an electrostatic change conferred by altering a methionine to an arginine residue. As a result, the recognized M protein population might represent free M protein, while the unrecognized population could represent protein either (1) bound to other host/viral proteins, or (2) post-translationally modified at or near the 23H12 epitope.

In addition to the observed changes in post-translational modification of VSV P and M proteins, type I IFN-induced changes in G-protein isoelectric focusing patterns presented the possibility of altered VSV G-protein glycosylation. Since this was a side observation made in experiments designed to test other hypotheses, more work needs to be done to verify the nature and extent of these differences in G-protein pI. If IFN-induced changes in glycosylation are independently verified, the question of how such alterations affect affinity for the host cell receptor and fit into a possible role for viral misassembly would need to be addressed.

IFN action has previously been shown to affect viral assembly in other cell lines (e.g., fibroblasts and bone marrow/thymus cells) (57). Specifically, in fibroblasts an IFN-elicited reduction in the incorporation of VSV G and M into virions led to the generation of defective "bald" particles (41). In bone marrow/thymus cells infected with murine leukemia virus, a 10^3-fold decrease in infectious virions, independent of overall viral titers, was observed with little effect on viral transcript/protein production (57). These differences in IFN responses between such disparate host cells are not surprising considering the more than 300 IFN-stimulated genes (12), and the difference in terminal differentiation of these cells.

Contact between N and M is thought to be the primary interaction involved in encapsidation of RNP cores by budding virions (5,6), and any disruption of that interaction could be responsible for impaired viral assembly and egress. This finding could be correlated with M protein hyperphosphorylation, if such phosphorylation were at positions in M critical for viral protein-protein interactions involved in VSV assembly.

While the above experimental evidence points to hyperphosphorylation, in order to verify whether additional phosphorylation sites exist within VSV M to be targeted by type I IFN-induced kinases, the web-based program NetPhospho 2.0^{TM} was used to analyze the M protein primary structure (Table 1). NetPhospho 2.0-predicted sites were then cross-referenced with both experimental (35) and x-ray crystallographic (21) data to yield 19 putative sites that may account for the hyperphosphorylation phenomenon seen in M due to a type I IFN cellular response in neurons.

Interestingly, a predicted site for tyrosine phosphorylation was found within the PPPY late domain, a site implicated in mono-ubiquitination and shown to be vital for efficient

budding (18). Consistent with this idea, evidence is also beginning to emerge that points to IFN-induced responses countering viral late domain function. NEDD4, the E3-ligase whose activity has been shown to act in a PPPY-dependent manner, was recently found to be targeted and interfered with by ISG15-ylation (29).

Lastly, it will be interesting to see whether hypophosphorylation is responsible for the modest reduction in RDRP functions previously reported in type I IFN-treated neurons (52), or if hypophosphorylated P associated with RNP limits the budding of infectious particles. Equally interesting would be to determine which amino acids are involved in both the hypo- and hyperphosphorylation patterns observed. Ultimately, the regulation of cellular kinases and phosphatases by IFN, which contribute to its antiviral effects, will need to be explored. Elucidation of any kinases and/or phosphatases involved in this type I IFN response could determine whether this is a yet-to-be-identified general antiviral response in all cell types, or one specific to the neuronal lineage. The identification of any new mechanisms of IFN action may help to highlight novel therapeutic targets for efficacious immunomodulation that are vital for the treatment of viral encephalitis.

Acknowledgments

We gratefully thank Dr. Gail Wertz (University of Virginia) for the generous gift of anti-VSV P and anti-VSV N polyclonal antibodies, and Dr. Douglas S. Lyles (Bowman Gray Medical School) for the generous gift of the anti-M MAb 23H12, and Laurent Poliquin (University of Quebec) for the M51R construct. We also would like to thank Dr. Theresa Chang (Mount Sinai School of Medicine) for helpful discussions, as well as our colleagues Adam D. Botwinick and James M. Miller for providing preliminary work, additional editing, and input. This work was supported by grants from the NIH to C.S.R. (DC003536 and NS039746).

Author Disclosure Statement

P.M.D. conducted experiments and wrote the manuscript. J.J.A. conducted the experiments pertaining to MAb 23H12 affinity for wild-type and M51R mutated M protein. C.S.R. conceived the study, served as chief scientific advisor, and edited the manuscript. All authors read and approved the final manuscript. The authors declare that no conflicting financial interests exist.

References

1. Barik S, and Banerjee AK: Sequential phosphorylation of the phosphoprotein of vesicular stomatitis virus by cellular and viral protein kinases is essential for transcription activation. J Virol 1992;66:1109–1118.
2. Barr JN, Whelan SP, and Wertz GW: Transcriptional control of the RNA-dependent RNA polymerase of vesicular stomatitis virus. Biochim Biophys Acta 2002;1577:337–353.
3. Battcock SM, Collier TW, Zu D, and Hirasawa K: Negative regulation of the alpha interferon-induced antiviral response by the Ras/Raf/MEK pathway. J Virol 2006;80:4422–4430.
4. Chen M, Ogino T, and Banerjee K: Mapping and functional role of the self-association domain of vesicular stomatitis virus phosphoprotein. J Virol 2006;80:9511–9518.
5. Chong LD, and Rose JK: Membrane association of functional vesicular stomatitis virus matrix protein *in vivo*. J Virol 1993;67:407–414.
6. Chong LD, and Rose JK: Interactions of normal and mutant vesicular stomatitis virus matrix proteins with the plasma membrane and nucleocapsids. J Virol 1994;68:441–447.
7. Dafny N, and Yang PB: Interferon and the central nervous system. Eur J Pharmacol 2005;523:1–15.
8. Das SC, and Pattnaik AK: Phosphorylation of vesicular stomatitis virus phosphoprotein P is indispensable for virus growth. J Virol 2004;78:6420–6430.
9. Das SC, and Pattnaik AK: Role of the hypervariable hinge region of phosphoprotein P of vesicular stomatitis virus in viral RNA synthesis and assembly of infectious virus particles. J Virol 2005;79:8101–8112.
10. De BP, and Banerjee AK: Specific interactions of vesicular stomatitis virus L and NS proteins with heterologous genome ribonucleoprotein template lead to mRNA synthesis *in vitro*. J Virol 1984;51:628–634.
11. De BP, and Banerjee AK: Requirements and functions of vesicular stomatitis virus L and NS proteins in the transcription process *in vitro*. Biochem Biophys Res Commun 1985;126:40–49.
12. Der SD, Zhou A, Williams BR, and Silverman RH: Identification of genes differentially regulated by interferon alpha, beta, or gamma using oligonucleotide arrays. Proc Natl Acad Sci USA 199895:15623–15628.
13. Detje CN, Meyer T, Schmidt H, *et al.*: Local type I IFN receptor signaling protects against virus spread within the central nervous system. J Immunol 2009;182:2297–2304.
14. Durbin JE, Hackenmiller R, Simon MC, and Levy DE: Targeted disruption of the mouse Stat1 gene results in compromised innate immunity to viral disease. Cell 1996;84:443–450.
15. Emerson SU, and Yu Y: Both NS and L proteins are required for *in vitro* RNA synthesis by vesicular stomatitis virus. J Virol 1975;15:1348–1356.
16. Faria PA, Chakraborty P, Levay A, *et al.*: VSV disrupts the Rae1/mrnp41 mRNA nuclear export pathway. Mol Cell 2005;17:93–102.
17. Francoeur AM, Poliquin L, and Stanners CP: The isolation of interferon-inducing mutants of vesicular stomatitis virus with altered viral P function for the inhibition of total protein synthesis. Virology 1987;160:236–245.
18. Freed EO: Viral late domains. J Virol 2002;76:4679–4687.
19. Gao Y, and Lenard J: Multimerization and transcriptional activation of the phosphoprotein (P) of vesicular stomatitis virus by casein kinase-II. EMBO J 1995;14:1240–1247.
20. Garcia-Sastre A, and Biron CA: Type 1 interferons and the virus-host relationship: a lesson in detente. Science 2006;312: 879–882.
21. Gaudier M, Gaudin Y, and Knossow M: Crystal structure of vesicular stomatitis virus matrix protein. EMBO J 2002;21: 2886–2892.
22. Glodowski DR, Petersen JM, and Dahlberg JE: Complex nuclear localization signals in the matrix protein of vesicular stomatitis virus. J Biol Chem 2002;277:46864–46870.
23. Goodbourn S, Didcock L, and Randall RE: Interferons: cell signaling, immune modulation, antiviral response and virus countermeasures. J Gen Virol 2000;81:2341–2364.
24. Goodman D, and Matzura H: An improved method of counting radioactive acrylamide gels. Anal Biochem 1971;42: 481–486.
25. Green TJ, Macpherson S, Qiu S, Lebowitz J, Wertz GW, and Luo M: Study of the assembly of vesicular stomatitis virus N protein: role of the P protein. J Virol 2000;74:9515–9524.

26. Gupta AK, and Banerjee AK: Expression and purification of vesicular stomatitis virus N-P complex from *Escherichia coli:* role in genome RNA transcription and replication *in vitro*. J Virol 1997;71:4264–4271.
27. Harty RN, Brown ME, McGettigan JP, *et al.*: Rhabdoviruses and the cellular ubiquitin-proteasome system: a budding interaction. J Virol 2001;75:10623–10629.
28. Harty RN, Paragas J, Sudol M, and Palese P: A proline-rich motif within the matrix protein of vesicular stomatitis virus and rabies virus interacts with WW domains of cellular proteins: implications for viral budding. J Virol 199973:2921–2929.
29. Hsiang TY, Zhao C, and Krug RM: Interferon-induced ISG15 conjugation inhibits influenza A virus gene expression and replication in human cells. J Virol 2009;83:5971–5977.
30. Huang S, Hendriks W, Althage A, *et al.*: Immune response in mice that lack the interferon-gamma receptor. Science 1993;259:1742–1745.
31. Hwang LN, Englund N, Das T, Banerjee AK, and Pattnaik AK: Optimal replication activity of vesicular stomatitis virus RNA polymerase requires phosphorylation of a residue(s) at carboxy-terminal domain II of its accessory subunit, phosphoprotein P. J Virol 1999;73:5613–5620.
32. Ireland DD, and Reiss CS: Gene expression contributing to recruitment of circulating cells in response to vesicular stomatitis virus infection of the CNS. Viral Immunol 2006;19:536–545.
33. Jayakar HR, Jeetendra E, and Whitt MA: Rhabdovirus assembly and budding. Virus Res 2004;106:117–132.
34. Jayakar HR, Murti KG, and Whitt MA: Mutations in the PPPY motif of vesicular stomatitis virus matrix protein reduce virus budding by inhibiting a late step in virion release. J Virol 2000;74:9818–9827.
35. Kaptur PE, McKenzie MO, Wertz GW, and Lyles DS: Assembly functions of vesicular stomatitis virus matrix protein are not disrupted by mutations at major sites of phosphorylation. Virology 1995;206:894–903.
36. Katze MG, He Y, and Gale M Jr: Viruses and interferon: a fight for supremacy. Nat Rev Immunol 2002;2:675–687.
37. Kramer MJ, Dennin R, Kramer C, *et al.*: Cell and virus sensitivity studies with recombinant human alpha interferons. J Interferon Res 1983;3:425–435.
38. Lefrancois L, and Lyles DS: The interaction of antibody with the major surface glycoprotein of vesicular stomatitis virus. II. Monoclonal antibodies of non-neutralizing and cross-reactive epitopes of Indiana and New Jersey serotypes. Virology 1982;121:168–174.
39. Lichty BD, McBride H, Hanson S, and Bell JC: Matrix protein of vesicular stomatitis virus harbours a cryptic mitochondrial-targeting motif. J Gen Virol 2006;87:3379–3384.
40. Little LM, Zavada J, Der CJ, and Huang AS: Identity of HeLa cell determinants acquired by vesicular stomatitis virus with a tumor antigen. Science 1983;220:1069–1071.
41. Maheshwari RK, Demsey AE, Mohanty SB, and Friedman RM: Interferon-treated cells release vesicular stomatitis virus particles lacking glycoprotein spikes: correlation with biochemical data. Proc Natl Acad Sci USA 1980;77:2284–2287.
42. Masters PS, and Banerjee AK: Complex formation with vesicular stomatitis virus phosphoprotein NS prevents binding of nucleocapsid protein N to nonspecific RNA. J Virol 1988;62:2658–2664.
43. Muller U, Steinhoff U, Reis LF, Hemmi S, Pavlovic J, Zinkernagel RM, and Aguet M: Functional role of type I and type II interferons in antiviral defense. Science 1994;264:1918–1921.
44. Ogden JR, Pal R, and Wagner RR: Mapping regions of the matrix protein of vesicular stomatitis virus which bind to ribonucleocapsids, liposomes, and monoclonal antibodies. J Virol 1986;58:860–868.
45. Okumura A, Pitha PM, and Harty RN: ISG15 inhibits Ebola VP40 VLP budding in an L-domain-dependent manner by blocking Nedd4 ligase activity. Proc Natl Acad Sci USA 2008;105:3974–3979.
46. Perlman SM, and Huang AS: RNA synthesis of vesicular stomatitis virus. V. Interactions between transcription and replication. J Virol 1973;12:1395–1400.
47. Petersen JM, Her LS, Varvel V, Lund E, and Dahlberg JE: The matrix protein of vesicular stomatitis virus inhibits nucleocytoplasmic transport when it is in the nucleus and associated with nuclear pore complexes. Mol Cell Biol 2000;20:8590–8601.
48. Raiborg C, and Stenmark H: The ESCRT machinery in endosomal sorting of ubiquitylated membrane proteins. Nature 2009;458:445–452.
49. Shestakova E, Bandu MT, Doly J, and Bonnefoy E: Inhibition of histone deacetylation induces constitutive derepression of the beta interferon promoter and confers antiviral activity. J Virol 2001;75:3444–5342.
50. Taylor GM, Hanson PI, and Kielian M: Ubiquitin depletion and dominant-negative VPS4 inhibit rhabdovirus budding without affecting alphavirus budding. J Virol 2007;81:13631–13639.
51. Trottier MD, Lyles DS, and Reiss CS: Peripheral, but not central nervous system, type I interferon expression in mice in response to intranasal vesicular stomatitis virus infection. J Neurovirol 2007;13:433–445.
52. Trottier MDJ, Palian BM, and Shoshkes Reiss C: VSV replication in neurons is inhibited by type I IFN at multiple stages of infection. Virology 2005;333:215–225.
53. Truckenmiller ME, Tornatore C, Wright RD, Dillon-Carter O, Meiners S, Geller HM, and Freed WJ: A truncated SV40 large T antigen lacking the p53 binding domain overcomes p53-induced growth arrest and immortalizes primary mesencephalic cells. Cell Tissue Res 1998;291:175–189.
54. van den Broek MF, Muller U, Huang S, Aguet M, and Zinkernagel RM: Antiviral defense in mice lacking both alpha/beta and gamma interferon receptors. J Virol 1995;69:4792–4796.
55. Vogel SN, and Fertsch D: Macrophages from endotoxin-hyporesponsive (Lpsd) C3H/HeJ mice are permissive for vesicular stomatitis virus because of reduced levels of endogenous interferon: possible mechanism for natural resistance to virus infection. J Virol 1987;61:812–818.
56. Wertz GW, Whelan S, LeGrone A, and Ball LA: Extent of terminal complementarity modulates the balance between transcription and replication of vesicular stomatitis virus RNA. Proc Natl Acad Sci USA 1994;91:8587–8591.
57. Wong PK, Yuen PH, MacLeod R, Chang EH, Myers MW, and Friedman RM: The effect of interferon on *de novo* infection of Moloney murine leukemia virus. Cell 1977;10:245–252.

Address correspondence to:
Dr. Carol Shoshkes Reiss
Biology Department
New York University
100 Washington Square East
New York, NY 10003-6688

E-mail: carol.reiss@nyu.edu

Received June 29, 2009; accepted August 10, 2009.